치의과학박사 학위논문

Role of nitric oxide-releasing compound in soft tissue regeneration and osteogenesis

연조직 및 경조직 재생에서 일산화질소 복합체의 역할

2020년 8월

서울대학교 대학원

치의과학과 구강악안면외과학 전공

신 정 현

Role of nitric oxide-releasing compound in soft tissue regeneration and osteogenesis

지도교수 명 훈

이 논문을 치의과학박사 학위논문으로 제출함

2020년 05월

서울대학교 대학원

치의과학과 구강악안면외과학 전공

신 정 현

신정현의 박사 학위논문을 인준함

2020년 07월

위 원 장 김 성 민 (인)

부위원장 명 훈 (인)

위 원 박 영 석 (인)

위 원 윤 혜 정 (인)

위 원 김 지 은 (인)

-Abstract-

Role of nitric oxide-releasing compound in soft tissue regeneration and osteogenesis

Jung-Hyun Shin, D.D.S., M.S.D.

Program in Oral and Maxillofacial Surgery, Department of Dental Science, Graduate School, Seoul National University.

(Directed by Professor Hoon Myoung, D.D.S., M.S.D., Ph.D.)

Purpose

Tissue defects of the oral cavity are relatively common; however, its management is often challenging. Nitric oxide (NO)-releasing compound was reported to enhance wound healing by promoting re-epithelialization, angiogenesis, and osteoblast differentiation. The purpose of the study was to investigate the effects of NO-releasing compound in the tissue repair using synthetic agents and through *in vitro* and *in vivo* experiments.

Materials and methods

Synthetic NO-releasing compound consisting of pluronic F68, branched polyethylenimine and NONOates (FBN) was administrated in *Porphyromas gingivalis* (*P. gingivalis*) to evaluate antimicrobial effect. Also, scratch analysis was used to assess the migration of human gingival fibroblast-1 (HGF-1) treated with FBN. *In vivo* mouse experiments with a total of 33 BALB/C mice was performed to see effects of FBN on the mucosal defects of palate. To find the role of FBN in the repair of bone defect, 80 sprague-dawley rats with artificial calvarial defect were used in this study. Radiologic findings with micro-computed tomography (micro-CT) and histopathologic examination along with immunohistochemistry (IHC) were reviewed *in vivo* animal experiments.

Results

Although direct bactericidal effect of pluronic F68-branched polyethylenimine (FB) was not observed, growth of P. gingivalis was inhibited by FB compared to control. Bacteriostatic and bactericidal effect were observed for FBN at a lower concentration than FB. Also, higher migration rate was found in HGF-1 treated with FBN, and wound size of the palate was significantly decreased in FBN

treatment (all $p < 0.05$). According to immunohistochemical result, re-epithelialization and wound contraction tended to increase in the FBN-treated mucosal wounds. Bone volume and bone volume/tissue volume ratio were significantly higher among experimental groups treated with collagen sponges ($p < 0.05$). Immunohistochemical staining for CD31 and analysis of microvessel density (MVD) showed that angiogenesis was more prominent in the FBN-treated group.

Conclusions

FBN exerted an antimicrobial effects and enhanced migration of HGF-1 cells and palatal mucosal healing. In calvarial defect, FBN was demonstrated to promote osteogenesis when applied in combination with a collagen sponge. These data suggest that FBN can be applied to ulcerative mucosal lesion and can be applied with collagen sponge to bone defect that are not amenable to bone grafts.

Keywords: nitric oxide (NO), pluronic F63-BPEI-NONOates (FBN), soft tissue regeneration, osteogenesis

Student Number: 2015-30629

Contents

I. Introduction---------- 1

II. Review of literature---------- 7

1. NO---------- 7

2. NONOates---------- 9

3. Soft tisssue regerneration---------- 10

4. Osteogenesis---------- 14

III. Materials and Methods---------- 17

1. Synthesis of NO-releasing compound---------- 17

2. Measurement of NO release---------- 18

3. Bacterial cultivation---------- 18

4. Antimicrobial assays---------- 19

5. Scanning electron microscopy (SEM)---------- 20

6. Cytotoxicity by MTT assay---------- 21

7. Scratch assay---------- 22

8. Animal study: the effects of FBN on soft tissue healing in palatal wound mouse model---------- 22

9. Animal study: the effects of FBN on bone formation in calvarial defect rat model---------- 24

10. Micro-CT analysis---------- 26

11. Histology and IHC---------- 26

12. Statistical analysi ---------- 29

IV. Results---------- 30

1. No release kinetics from FBN---------- 30

2. Antimicrobial activity of FBN----------30

3. Bacterial morphology observed by SEM----------31

4. Cytotoxicity to HGF-1 cells----------31

5. Scratch assay----------32

6. Evaluation of wound healing assay----------32

7. Histology and IHC for evaluation of wound healing-----33

8. Evaluation of micro-CT in calvarial defect rat model---34

9. Histology for evaluation of bone formation Formation in calvarial defect rat model----------36

V. Discussion ----------39

VI. Conclusions----------51

References---------- 53

Tables---------- 73

Figures legends and Figures----------78

Abstract in Korean----------99

I. Introduction

Nitric oxide (NO) is a highly reactive gaseous molecule in mammalian cell[1]. NO plays essential roles in biological reactions such as cell differentiation, immune response, angiogenesis, vasodilation, and inflammatory response, and also exerts a strong bactericidal effect against various bacteria[2]. Additionally, NO functions to promote wound healing through re-epithelialization and collagen deposition[3,4]. In addition to the NO molecule, reactive oxygen intermediates exhibit broad-spectrum antibacterial activity by influencing the deamination of DNA, breakage of DNA strands, and peroxidation of lipids[5]. NO delivery tools such as NONOates have been developed that can store and release NO[6]. NONOates are used widely to deliver exogenous NO and can be easily synthesized through the treatment of secondary amine groups with NO gas, where 1 mol of NONOates releases 2 moles of NO instantaneously[7]. Various materials possessing secondary amines can be functionalized into NONOates. Pluronic F68 is a water-soluble and thermosensitive triblock copolymer that can be used as a support scaffold[8]. This molecule acts as a surfactant with good biocompatibility and has been approved by Food and Drug Administration[9,10]. In a previous study,

treatment with a NO-releasing system that was synthetized by conjugating NONOates into branched polyethylenimine (BPEI) that was linked with pluronic F68 resulted in enhancement of endothelial cells[11], re-epithelialization, blood vessel formation, collagen deposition[12] and excellent antibacterial activity with low cytotoxicity[13]. Macromolecular NO donors such as F68-BPEI-NONOates (FBN) exhibit improved antibacterial activity compared to that of small-molecule NO donors[14].

Wound healing is a biological process that is controlled by complex mechanisms[15]. During the process of wound healing, all tissues follow the same mechanism that includes inflammation, proliferation, and remodeling phases[16]. The inflammatory phase begins after hemostasis[16,17]. During this phase, pathogens are eliminated, and cytokines, leukocytes, macrophages, and granulocytes play important roles[18]. The wound area is reduced by contraction at the proliferation phase[19]. Fibroblasts are located at the edge of the wound, and circulating mesenchymal progenitor cells proliferate at the wound site[20]. Oxygen and nutrients are supplied to fibroblasts through re-vascularization[21]. During the remodeling phase, the extracellular matrix is reorganized, degraded, and resynthesized, and the

maximum tensile strength is subsequently increased while the wound matures. The oral cavity possesses a unique environment that contains millions of microbes and warm saliva[17]. The wound healing process may require a longer period of time in this environment, and wound infections also often result in the formation of ulcers[4]. Oral mucosal diseases include oral mucositis caused by radiation or chemotherapy in patients with oral cancer, recurrent aphthous stomatitis, and oral mucosal ulcers caused by dentures in elderly patients. There are several treatment modalities for oral mucosal disease. Chlorhexidine can reduce the duration of oral mucosal lesions and decrease ulceration. However, chlorhexidine disinfects the wounds of the oral mucosa and is not an agent that promotes wound healing. Non-corticosteroid-based molecules can act to relieve pain associated with oral mucosal diseases, but these drugs cannot regenerate the oral mucosa. Corticosteroids suppress inflammatory and immune responses. By inhibiting the production of bradykinin and histamine, these drugs reduce capillary permeability and inhibit white blood cells from travelling to the site of inflammation. They also inhibit formation of granulation tissue by inhibiting fibroblast proliferation and angiogenesis, and they reduce cytokine

and tumor necrosis factor−α (TNF−α) and decrease the activity of macrophages. However, although corticosteroids exert a strong anti−inflammatory effect in the early stage, they can damage the mucosal barrier when repeatedly used for long periods of time[22]. The current methods for treating oral mucosal diseases can cause side effects, and most of these methods are only designed for symptom relief. During the inflammation stage, NO increases antiplatelet effects and vasodilation. During the proliferative phage, NO increases angiogenesis and re−epithelialization, and during the remodeling phage, NO increases collagen deposition[23]. NO can be developed as a biocompatible molecule for wound healing of the oral cavity.

Bone grafts are necessary if there is vertical or horizontal bone loss. Bone formation in the oral cavity has difficulties due to factors such as the wet environment caused by saliva, the possibility of infection by bacteria, wound irritation caused by mastication, and increased tension resulting from muscular contractions. Based on this, it is necessary to develop substances such as bone morphogenetic protein−2 (BMP−2) that can induce bone formation. NO exerts various effects on bone formation. At low concentrations, NO suppresses bone absorption by osteoclasts and promotes the growth

of osteoblasts; however, at high concentrations NO results in the opposite effects[24]. NO therapy can be used to prevent bone loss after menopause[25]. A number of studies have been conducted to examine the efficacy of NO in postmenopausal women who cannot afford hormone replacement therapy. Bone mineral density (BMD) was increased when nitroglycerin was administered as a donor of nitric oxide. NO donors such as nitroglycerin, nitrates, and glyceryl trinitrate are used for clinical treatment, and they are safe and effective drugs[26]. It is believed that the local application of NO may also induce the formation of bone in the context of bone defects. Based on this and the ability of NO to control bone metabolism, it will be of value to study this molecule as a potential bone stimulant in the context of bone defects.

As NO possesses characteristics that include antibacterial effects, angiogenesis promotion, and vasodilation, this molecule may be useful in the context of both hard and soft tissue defects. Based on this, the purpose of this study was to evaluate the biocompatibility of NO-releasing compound by measuring the cytotoxicity and antibacterial action of FBN and to evaluate if it promotes wound regeneration in soft tissue wounds and osteogenesis in hard tissue

defects. To assess the effect of NO on soft tissue wound healing and bone formation, cytotoxicity, migration, and wound healing assays, micro-computed tomography analyses, and immunohistochemistry (IHC) studies were performed.

II. Review of literature

1. NO

Prior to the 1980s, NO was considered to be an air pollutant produced by automotive exhaust and industrial processes. Murad *et al.*, Furchgott *et al.*, and Ignarro *et al.* independently discovered that NO functions as an endothelial-derived relaxation factor[27-29]. Following this discovery, a great deal of research has been performed to examine the functions of NO as a signaling molecule[30]. Various biological functions of NO were discovered and these included roles in apoptosis[31], neurotransmission[26], immune response[32], cardiovascular homeostasis[33], and angiogenesis[34]. The endogenous NO molecule is formed by oxidation and cleavage of L-arginine through the catalytic properties of NO synthases (NOS). The reaction requires oxygen and electrons from nicotinamide adenine dinucleotide phosphate (NADPH), and the co-product (L-citrulline) is ultimately produced. There are three types of NO synthetases that synthesize NO[26]. NO synthetases include the neuronal form isolated from the brain (type 1; nNOS), the inducible form isolated from murine macrophages (Type 2; iNOS) and the endothelial form

isolated from small aortic endothelial cells (Type 3; eNOS)[35,36]. During soft tissue wound healing, NO has been found to promote re-epithelialization, angiogenesis, collagen deposition, and keratinocyte formation[37,38]. Reactive nitrogen/oxygen species that are produced by high concentrations of NO cause apoptosis by promoting deamination of DNA, structural changes in proteins, and inflammatory reactions. NO and its intermediates exhibit antibacterial activity by facilitating the deamination of bacterial DNA and lipid peroxidation[31,32]. NO promotes osteoblast differentiation at low concentrations and inhibits osteoclasts, and this molecule exerts the opposite actions at high concentrations. Bone metabolism is regulated by NO through the NO/cyclic guanosine monophosphate pathway (cGMP)[25,39]. Bone remodeling and resorption are important processes that are required to repair bone damage. NO possesses anabolic action in the context of osteogenesis[25]. A number of previous studies have indicated that nitroglycerin and nitrate act as NO donors to increase BMD[39,40]. The various functions of NO are determined by the concentration and duration of NO release[41]. NO-releasing compounds have been developed for use as therapeutic agents for these functions. Donors of NO include metal-NO complexes, S-

nitrosothiols, organic nitrates, nitrites, nitrobenzene, and NONOates[42,43]. NO-releasing compounds have also been produced by surface coating and nanotechnology. However, one major problem with the existing NO-releasing compounds is that it is difficult to finely adjust their concentrations. During storage, these compounds undergo unintended reactions with various atoms and molecules. NO should not be released during storage and should instead be released at a desired time.

2. NONOates

The chemical structure of NONOates consists of two negatively charged oxygen atoms and a positively charged N=N group[41]. NONOates are classified into two categories that include C-bound and N-bound. The N-bound type is the most widely used NO-releasing compound type[32]. N-bound NONOates can be functionalized to secondary amines. NONOates release NO through spontaneous decomposition by acid-catalyst reactions. In one functional group, NONOates produce 2 moles of NO per 1 mole of compound[33]. The release of NO without metabolites is an important

advantage over other NO-releasing compounds. NONOates can be easily synthesized with 80 psi of NO in a high pressure reactor for 3 days. NO release kinetics of NONOates can be diversified according to parent molecules[11]. C-bound NONOates such as alanosine, dopatin, and fragin are found in nature[44].

3. Soft tissue regeneration

The wounds of the oral mucosa and skin undergo a healing process that involves hemostasis, inflammation, proliferation, and remodeling. Hemostasis begins with platelet aggregation and thrombus formation to prevent blood loss. Platelets secrete granules of several growth factors, including transforming growth factor-β (TGF-β), epidermal growth factor (EGF), and insulin-like growth factor -1 (IGF-1). These factors activate endothelial cells, macrophages, and neutrophils to initiate a wound healing cascade. Clots composed of fibronectin, fibrin, and vitronectin act as a matrix for cell migration. Serotonin is released from platelets to increase microvascular permeability. Tissue edema is caused by fluid that is discharged into the extravascular space[45,46]. Inflammation begins with the onset of

this cascade and the activation of complement. Platelets, TGF-β, and complement stimulate the migration of polymorphonuclear leukocyte (PMNL) within 24 hours of injury. PMNL moves to and adheres to vascular endothelial cells by migration, and it then moves through the walls of blood vessels. PMNL eliminates exogenous substances by producing proteolytic enzymes and reactive oxygen species. During the late inflammatory phase, monocytes migrate to the wound site in response to chemoattractants such as cytokines, growth factors, inflammatory mediators, and immunoglobulins. At 48-72 hours, monocytes become macrophages. Macrophages produce growth factors that induce extracellular matrix (ECM) production and the proliferation of smooth muscle and endothelial cells. Macrophages also secrete matrix metalloproteinases (MMPs)[47]. Proliferation occurs rapidly in response to damage. Keratinocytes at the edge of the wound proliferate 12 hours after the initial wound. When keratinocytes meet, their movement stops and a basement membrane is formed. As epithelial cells grow and differentiate, the stratified epithelium is produced. Keratinocyte growth factor, EGF, and basic fibroblast growth factor (bFGF) stimulate keratinocyte proliferation and mitogenesis to regulate epithelialization[48].

Fibroblasts migrate to the wound site 2–4 days after wounding in response to TGF-β and platelet-derived growth factor (PDGF). Fibroblasts are in a quiescent state in the intact area; however, they exhibit a high rate of proliferation at the wound area. Fibroblasts play a role in granulation tissue formation and ECM reorganization. Initially, collagen is highly disordered, and the remodeling of the ECM is facilitated by MMPs. Continual remodeling occurs, and collagen deposits and vascular density decrease. Blood flow and metabolic activity also decrease. Granulation tissue matures along with collagen, ECM, elastic tissue, and spindle-shaped fibroblasts. Hyaluronan and fibronectin are degraded, and collagen diameter increases[49,50].

The oral mucosa exhibits several differences when compared to the skin. The oral mucosa consists of an epithelial layer, a basal lamina, a lamina propria, and a submucosal layer. The submucosal layer does not exist in the gingiva and palate. The lamina propria attaches directly to the bone, and this is known as the mucoperiosteum[51]. The gingiva and palatal mucosa are composed of keratinized epithelium that can resist mechanical forces. The tongue is a parakeratinized epithelium consisting of keratinized and non-keratinized epithelium[52]. The non-keratinized mucosa possesses a loose ECM structure, and

the keratinized mucosa exhibits an ECM structure similar to that of the skin[53]. The epithelium of the oral mucosa is thicker than the epidermis of the skin[54]. There are sweat glands, sebaceous glands, and hair follicles on the skin, and there are salivary glands on the oral mucosa. Compared to dermal keratinocytes, oral keratinocytes produce interleukin (IL)-6 more rapidly in response to TNF-α and IL-4. IL-1α induces IL-8 production in oral keratinocytes; however, it does not induce IL-8 production in dermal keratinocytes[55]. Endothelial progenitor cells (EPCs) are derived from the bone marrow and contribute to blood vessel formation during wound healing. EPCs have been demonstrated to improve re-epithelialization, angiogenesis, and macrophage recruitment in mouse models[56]. The number of blood vessels in the oral mucosa and skin was observed to be similar[57]. Vascular endothelial growth factor (VEGF) was similarly observed in intact oral mucosa and skin; however, VEGF levels were higher in injured skin than in injured mucosa[58]. ECM allows for cell attachment, acts as a barrier to foreign substances, and provides structural support. Collagen exists in 28 isoforms and is the most abundant ECM protein[59]. The diameter of fibrils was similar in wounded and intact oral mucosa[60]. The number

of procollagen type I was higher in skin wounds than in oral mucosal wounds[54].

4. Osteogenesis

During the process of osteogenesis, bone defects follow a mechanism that includes clot formation, inflammation, angiogenesis, migration and proliferation of mesenchymal stem cells and fibroblasts, bone formation, and a remodeling phase. Within 24 hours after injury, a blood clot is formed, and growth factors and cytokines are released to attract macrophages and neutrophils. Blood clots are absorbed and replaced with granular tissue that contains a large number of blood vessels. These vessels supply nutrients and mesenchymal stem cells that contribute to osteoid formation. Osteoid is ossified to form woven bones[61], and lamellar bone is also formed in this osteoid[62]. Primary sponge bone is replaced by reticular and compact bone. This series of processes occurs over three to four months[63]. Osteogenesis occurs when osteoprogenitor cells are present in grafted bone. Osteoprogenitor cells differentiate into osteoblasts that can form bone. Osteoinduction is the ability to stimulate undifferentiated stem

cells in surrounding tissues. These stem cells differentiate into osteoblasts that can induce bone formation. Osteoconduction cannot directly form bones and cannot respond to stimuli; however, this process possesses the ability to form new bone by creep replacement. The bone material includes autogenous bone, allogeneic bone, xenogeneic bone, and synthetic bone. Autologous bone is the most ideal graft and contains osteoprogenitor cells capable of osteogenesis, osteoinduction, and osteoconduction. It should be noted that additional surgery is required to provide bone grafts. Synthetic bones are similar in structure and composition to human bones; however, they exhibit less bone-forming ability. In allogeneic bone, antigens can cause problems[64]. Research has also been conducted to examine certain growth factors that are known to regulate the healing process. These growth factors include PDGF, IGF, bFGF, and TGF-α and -β. BMP-2 represents a group of transforming growth factors that has been used most frequently to promote bone formation in bone grafts. BMP-2 is a bone-forming protein that can induce stem cells to differentiate into osteoblasts. However, many side effects have been reported in response to BMP-2. Clinical side effects include induction of inflammation, radiculopathy, ectopic bone, osteoclast

activation, osteolysis, subsidence, hematoma, wound dehiscence, and infection[65]. It has also been reported that fibroblast growth factor-2 (FGF-2) can differentiate and proliferate various cells, induce angiogenesis, and promote bone formation. However, FGF-2 can cause excessive cellular proliferation and can activate anti-apoptotic pathways to promote carcinogenesis[66]. Although growth factors possess advantages such as their ability to induce osteoblast differentiation and promote angiogenesis, they have not been approved by the FDA due to various risk factors. BMP-2 is the only growth factor that can currently be used for osteogenesis.

III. Materials and Methods

1. Synthesis of NO-releasing compound

FBN was synthesized according to a previously reported method[13]. Briefly, 10 g of pluronic F68 in dichloromethane (DCM) (Sigma-Aldrich, St. Louis, MO, USA) was added dropwise to 1.2 g of p-nitrophenyl Chloroformate (pNPC) containing DCM. After stirring for 24 h, pNPC-conjugated pluronic F68 (pNPC-F68) was purified by precipitating with the addition of cold diethyl ether and then dried at room temperature. Next, 572 mg of BPEI and 1 ml of TEA in DCM was added to 3 g of pNPC-F68 at room temperature. After dissolving in distilled water, the product was dialyzed using a Spectra/Por dialysis membrane to remove the unreacted BPEI. Subsequent F68-BPEI (FB) was synthesized. For synthesizing FBN, 200 mg of FB was added to 30 wt% of sodium methoxide, 20 ml of dry methanol (0.5 M), and 3 ml of tetrahydrofuran. This product was placed in a high pressure NO reactor purged with argon gas. This reactor was filled with NO gas and maintained at 80 psi for 3 days. The solution was dried and precipitated with an excess of cold diethyl ether. The final product was stored at −20℃. The structures of FB and FBN are

shown in Fig. 1.

2. Measurement of NO release

Quantitative NO release was measured using a nitric oxide analyzer (Sievers 280i, Boulder, USA) that analyses the released NO. This equipment functions on the basis of a chemiluminescence reaction. A total of 0.5 mg of FBN was dissolved in 40 ml of Dulbecco's phosphate buffered saline. The release profile was measured at levels up to its detection limit (1 pmol) according to various NO parameters, including $[NO]_t$ (total nanomoles of NO released per mg, nmol/mg), $[NO]_m$ (maximum instantaneous concentration of NO released, pmol/mg/sec), t_m (time required to reach $[NO]_m$, min), and $t_{1/2}$ (half-life of NO release, min) and t_d (duration of NO above 1 pmol/s, h).

3. Bacterial cultivation

Porphyromonas gingivalis (*P. gingivalis*) (ATCC 33277, American Type Culture Collection, Manassas, VA) was cultured in brain heart infusion (BHI) broth containing hemin (1 μg/ml) and vitamin K (0.2

μg/ml) at 37°C under anaerobic conditions. *P. gingivalis* was then brought to a concentration of 1 × 10^7 cells/ml using fresh medium, and the number of bacteria was measured with a bacterial counting chamber (Lauda Konigshofen, Marienfeld, Germany).

4. Antimicrobial Assays

A total of 180 μl of BHI broth containing vitamin K and hemin was dispensed into 96-well plates (SPL Life Sciences, Gyeonggi-do). Appropriate concentrations of FB and FBN were added to 96-well plates, respectively. These compounds were diluted in 2-fold and added serially. The first column was used as a control by adding only broth. Next, a 20 μl bacterial suspension (containing 1 × 10^7 cells) was added to each well. This plate was incubated for 36 hours at 37℃ under anaerobic conditions. To assess bacterial growth, optical density was measured at a wavelength of 660 nm using a microplate reader (SpectraMax M2, Molecular Devices, Sunnyvale, USA). To evaluate the minimum inhibitory concentration (MIC), the minimum concentration required to prevent visible bacterial growth was measured. To evaluate the minimum bactericidal concentration

(MBC), 50 μl of liquid from each well was dispensed into trypticase soybean agar containing hemin, sheep blood, and vitamin K. These mixtures were incubated for 5 days at 37℃ under anaerobic conditions to allow for measurement of the lowest concentration without bacterial growth.

5. Scanning electron microscopy (SEM)

Bacterial culture was performed as mentioned previously. After centrifuging the tube at 4000 rpm for 10 minutes, the supernatant was aspirated. The content was suspended in distilled water (2 ml), and 1 ml of the solution was then transferred to a 24-well plate. FBN was added to the bacterial solution to adjust the final concentration to 1 mM. Then, the bacterial solution was incubated at 37℃ for 4 hours. Primary fixation of bacteria was performed at 4℃ for 24 hours using Karnovsky fixative consisting of 2% glutaraldehyde and 2% paraformaldehyde in 0.05 M sodium cacodylate buffer. This solution was washed three times for 10 minutes at 4℃ using the same buffer. Secondary fixation was performed using 2.5% glutaraldehyde in 0.05 M sodium cacodylate buffer (pH 7.2) for 2 hours. After dehydration

using an ethanol series, the specimens were freeze-dried (Hitachi ES-2030, Hitachi, Japan) and coated using an ion coater (Eiko IB-5; Eiko). The morphology of the bacteria was observed by SEM (Hitachi S-4500; Hitachi).

6. Cytotoxicity by MTT assay

The human gingival fibroblast (HGF)-1 (ATCC #CRL-2014) cell line was cultured in Dulbecco's modified Eagle's medium (DMEM). Cells with medium (100 μl) were seeded in 96-well plates (SPL Life Sciences) at a density of 1×10^4 cells/well and incubated for 24 h at 37° C. The culture medium was then removed. Control, 2 mM of FB, and 1 mM of FBN medium (100 μl) that was prepared in DEME were each added. The cells were then incubated for 24 h at 37° C. MTT solution (20 μl, 5 mg/ml) was added to each well and incubated for 4 h in the dark. The medium was removed, and dimethyl sulfoxide (DMSO, 100 μl) was added into each well to dissolve the formazan. The absorption was measured at a wavelength of 570 nm using a microplate reader (VERSAmax Tunable Microplate reader, Molecular Devices, CA, USA). The cell viability in each well was

compared to that in the untreated control (100%).

7. Scratch analysis

Scratch analysis was used to assess the migration of HGF-1 treated with PBS and FBN (1 mM, 0.05 mM, and 0.01 mM). Each well was scratched with a 1000- μL pipette tip to create a gap. The scratches were imaged by phase contrast microscopy. Images were acquired at 0 and 24 hours after scratching using contrast phase microscopy (magnification, ×100). A digital image analysis program (ImageJ®, National Institutes of Health, Bethesda, Maryland, USA) was used to assess the cell migration rate over time. The percentage of migration was calculated for each condition.

8. Animal study: the effects of FBN on soft tissue healing in palatal wound mouse model

This study was conducted following the protocol approved by The Korean University Medical Center Laboratory Animal Research Ethics Committee (KOREA-2017-0180-C1). All experiments were

conducted according to "Recommendations for Handling Laboratory Animals for Biomedical Research" in compliance with Korea University's Laboratory Safety and Ethics Handling Committee. Male BALB/C mice (11–12 weeks old) were used for this study. The mice were randomly divided into three groups (control, FB, and FBN) comprising eleven animals each. The animals were injected with alfaxalone (50 mg/kg) and xylazine (10 mg/kg) for anesthetizing. The mice were positioned in a supine orientation prior to use of an electric cauterizer. A 5 mm portion of the palatal mucosa was removed in the middle of the palate to the extent that the palatal bone was not exposed. The solutions (Control, 0.01 mM FB, and 0.01 mM FBN) were then prepared. Next, the solutions were applied to the wound for 5 days. PBS was used for the control group. As NO inhibits platelet aggregation[67], NO was applied one day after surgery. To prevent intake of the solution, the mouth was opened using a rodent mouth gag, and a gauze was placed in the posterior area of the palate. One mouse was sacrificed in each group at 7 and 14 days after wound formation for use in IHC. The remaining mice were sacrificed 14 days after wound formation. Palatal wounds were photographed using a COOLPIX S6500 camera on days 0, 7, and 14. A digital image analysis

program (ImageJ®, National Institutes of Health, Bethesda, Maryland, USA) was used to compare the wounds. Additionally, the tissues in the palatal area were obtained for histology and IHC analyses. Wound healing was measured as a percentage area of initial wound size[68]. A time table of the study design is shown in Fig. 2.A.

9. Animal study: the effects of FBN on bone formation in calvarial defect rat model

A total of 80 male Sprague-Dawley Rats (11-12 weeks old) that were acclimated for 1 week was used. The rats were maintained under a 12h-12h light-dark cycle at 22°C and provided water and food (rodent chow). Alfaxalone (10 mg/kg) and xylazine (5 mg/kg) were injected intraperitoneally for general anesthesia. The rat calvaria area was shaved and cleaned with povidone. After local anesthesia with lidocaine, longitudinal incisions from the nasal to occipital area in rat calvaria were performed. Then, a full-thickness mucoperiosteal flap was formed to expose the calvaria. After the skin and periosteum were separated from the calvaria, a dental core drill (5.5 mm in diameter; Osstem®, Korea) was used to create full-

thickness calvarial defects on the left and right sides. Critical defects of 5 mm in size are the smallest defects in which bone does not spontaneously regenerate[69]. The surgery was performed carefully so as to not damage the dura meter. Absorbable collagen sponges (ACS, Teruplug; Terumo Co., Tokyo, Japan) and bone particles (OSTEON^{TM} III, dentium, South Korea) with PBS, 0.05 mM FB, 0.05 mM FBN, or 0.01 mM FBN were used to fill in the defects (Fig. 3). The surgical sites were then covered with membranes (Genoses^{TM}, Dentium, South Korea) and sutured with 3-0 vicyl®. All rats received ampicillin for 5 days (263 mg/dl in water). Half of the rats were sacrificed at 4 weeks after surgery in each group, and the other half were sacrificed at 8 weeks after the surgery using 100% carbon dioxide. The calvaria were removed from the bodies. These specimens were fixed with 4% paraformaldehyde. Bone volume fractions (BV/TV, %) were measured to evaluate the amount of bone formation in the hematoxylin and eosin (H&E) slides from the 4-week and 8-week groups. Among the rats sacrificed at 4 weeks and 8 weeks after the surgery, IHC was performed using tissue from one rat from each group. The timeline of this experiment is described in Fig. 2.B.

10. Micro-CT analysis

The samples were scanned using a micro-CT (SkyScan 1173, Kontich, Belgium). The scanning conditions were as follows: voltage: 130 kV, current: 60 μA, duration of exposure: 500 ms, exposure range of 1 degree, Al filter: 1 mm, 40% beam hardening correction, and pixel size: 35.15 μm. Three-dimensional images were reconstructed using NRecon software. In each sample, bone volume (BV, mm^3), tissue volume (TV, mm^3), bone volume fraction (BV/TV, %), trabecular thickness (Tb Th, mm), trabecular separation (Tb Sp, mm), and trabecular number (Tb N, N/mm) were measured.

11. Histology and IHC

To evaluate the histopathologic changes (re-epithelialization and wound contraction) at mucosal wound area, H&E staining and immunohistochemical staining for cytokeratin-14 (CK-14) and α-smooth muscle actin (α-SMA) were performed. For the calvarial defect model, H&E staining was used to assess bone formation and cluster of differentiation-31 (CD-31) staining was used to assess

blood vessel formation.

The specimens were fixed in 10% neutral buffered formalin. Demineralization was performed using 10% EDTA (Chelatocal, National diagnostics, 305 Patton Drive Atlanta, Georgia 30336, USA). The demineralized tissue samples were dehydrated using increasing ethanol concentrations (70% to 100%), and the specimens were then embedded in paraffin. The blocks were sequentially sectioned to a 4 μm thickness. The slides were incubated at 65℃ for 30 minutes, deparaffinized using xylene, rehydrated by serial dilutions with alcohol (3 min, 3 times at 72℃), and washed with PBS (5 min). The slides were stained with H&E solution, dehydrated in alcohol, cleared in xylene, and then mounted.

For IHC, the primary antibodies, IHC detection systems, and antigen retrieval used for immunohistochemical analyses are shown in Table 1. IHC analyses were performed using an horseradish peroxidase (HRP) polymer detection kit (Ventana medical system, INC., AZ, USA) with a monoclonal antibody against CK-14 (1:400; Novocastra, NC, UK), α-SMA (1:800; NeoMarkers, CA, USA), and CD-31(1:200; Abcam, CB, UK). Heat-induced epitope retrieval was performed for 30 minutes in a water bath at 98℃ using a citrate

buffer solution (Vector Laboratories, USA) at pH 6.0. Blocking of endogenous enzymes was performed for 10 minutes using methanol (Sigma-Aldrich, USA) containing with 3% hydrogen peroxide solution (Panreac, Spain). The slides were incubated with primary antibodies for 30 minutes, and this was followed by incubation with the labelled polymer for 30 minutes. The slides were incubated for 10 minutes with 3,3'-diamino-benzidine (DAB) to visualize the reaction and then counterstained with Mayer' s hematoxylin. The slides were coverslipped (Mounting Medium, Richard Allan Scientific, USA) after dehydration. Histomorphologic measurements were acquired using Panoramic 250 Flash III from 3D Histech (No. 3 Öv Street Budapest, HUNGARY), and optical images were obtained using Caseviewer (ver.2.0, 3D Histech, HUNGARY). Semiquantitative analyses were conducted for CK-14 and α-SMA using tissue slides at 400X magnification. The staining intensity was divided into 4 groups (0, 1, 2, and 3). The percentage of positive cells was categorized into 4 groups (0: 0, 1: ≤25%, 2: =25-50%, and 3: ≥ 50%). The score was calculated by multiplying the staining intensity and percentage of positive cells. The score ranged from 0 to 9, and this was divided into 4 groups (Negative: 0, Low positive: 1-2,

Positive: 3-4, and High positive: 6-9)[70]. For CD31 staining, the number of microvessels was counted at 400X magnification according to the method of Weidner *et al.*[71]. This histological area was 221.432 μm^2. microvessel density (MVD, microvessel/mm^2) was then calculated.

12. Statistical analysis

To assess cytotoxicity to HGF-1 cells, the Mann-Whitney U test was used to evaluate the statistical differences between groups. To evaluate the scratch analysis results, the wound healing assay, the micro-CT, and the histology of bone formation assays, the statistical differences between groups were assessed using a one-way ANOVA followed by post-hoc Tukey's multiple comparison. The Kruskal-Wallis test followed by the Bonferroni's method was used for data that does not follow a normal distribution. The data are shown as mean ± standard deviation (SD) and $p < 0.05$ was considered to indicate statistical significance. The data were evaluated using SPSS software (version 23) (IBM Corp., Armonk, NY, USA).

IV. Results

1. No release kinetics from FBN

The release of NO from FBN was measured using a chemiluminescence NO analyzer in DPBS at 37°C. The NO release characteristics of FBN were recorded (Table 2). Fig. 4 shows changes in NO concentration over time and the cumulative NO release. The maximum instantaneous concentration was 117.5 pmol/mg at 11.2 min. The half-life of NO release was 53.1 min. The duration of NO release was 8.03 hours. The total number of nanomoles of NO release was 415 nmol/mg.

2. Antimicrobial activity of FBN

The minimum concentration of NO-releasing compounds required to inhibit the growth of *P. gingivalis* is 0.5 mM for FBN and 1 mM for FB. FBN inhibited bacterial growth at a lower concentration than FB. Additionally, MBC was measured to analyze the bactericidal effect. The MBC of FBN against *P. gingivalis* was measured at 1 mM. However, no bactericidal effect was observed for FB (Fig. 5).

3. Bacterial morphology observed by SEM

The morphology of bacteria was observed by SEM. Positive charges and NO can kill the bacteria by destroying the bacterial membrane. Peroxynitrite ($ONOO^-$) is a reactive intermediate produced by the reaction between NO and peroxide. $ONOO^-$ causes peroxidation of lipids in bacteria and destroys DNA strands. Destruction of the bacterial membrane treated with FBN was observed in the SEM images (Fig. 6).

4. Cytotoxicity to HGF-1 cells

The analysis of cell viability in response to treatments with NO-releasing compounds is based on the amount by which the formazan changes to tetrazolium through reductase activity. Using these analyses, the effective antibacterial concentrations of NO were measured as 2 mM and 1 mM for FB and FBN, respectively, and the cell viability was 77.95 ± 2.08% and 89.96 ± 1.84%, respectively (Fig. 7). These differences were statistically significant (p = 0.0004).

5. Scratch analysis

We assessed the effects of FBN on the migration of HGF-1 cells using scratch assays (Fig. 8). Scratch assays measured the area that was covered 24 hours after a scratch was created. The averages of migration rate were 43.01 ± 1.33%, 44.11 ± 1.20%, 49.07 ± 1.15%, and 57.98 ± 1.74%, respectively, in the control, 1 mM FBN, 0.05 mM FBN, and 0.01 mM FBN groups (Fig. 9). There was a statistically significant difference between the control and the 0.05 mM FBN groups, the control and the 0.01 mM FBN groups, the 1 mM FBN and 0.01 mM FBN groups, and the 0.05 mM FBN and 0.01 mM FBN groups, respectively ($p = 0.0183$, $p < 0.0001$, $p < 0.0001$, and $p = 0.0003$). The migration rate was highest in the 0.01 mM FBN group.

6. Evaluation of wound healing assay

To evaluate the wound healing effects of FB (0.01 mM) and FBN (0.01 mM), the area ratio of wound healing was calculated by measuring the area of the wound on the day of surgery and at 7 and 14 days after surgery. Representative wounds from each group at

days 7 and 14 are shown in Fig. 10. At 7 days, the wound healing rates in each group were 35.4 ± 1.62%, 39.5 ± 1.82%, and 50.8 ± 1.42% for the control, FB, and FBN groups, respectively. At 14 days, the wound healing rates in each group were 42.0 ± 2.39%, 48.2 ± 1.60%, and 60.2 ± 1.12% for the control, FB, and FBN groups, respectively. (Fig. 11) On day 7 and 14, wound healing was significantly increased in the FBN-treated group compared to that in the other groups ($p < 0.05$ for control group, FB group). No significant infection or weight loss was observed in mice during the study.

7. Histology and IHC for evaluation of wound healing.

According to H&E staining, re-epithelialization was further increased in the FBN group on day 7. On day 14, mucosal remodeling was observed in all groups. In particular, re-epithelialization was achieved according to the observation of well differentiated epithelium in the FBN group (Fig. 12). CK-14 staining revealed all groups to be highly positive according to semiquantitative analyses. There was no difference in the intensity of staining among the groups;

however, the extent of staining was observed to be greater, and re-epithelialization was increased in FBN group. The deposition of CK-14 throughout the entire layer of epithelium was observed in the FBN group (Fig. 12, 13). α-SMA staining revealed weakly positive results for the control group on day 7. The FB group on day 7 and the control and FB groups on day 14 were determined to be positive, and the FBN group on days 7 and 14 was determined to be strongly positive. On days 7 and 14, a higher level of α-SMA was observed in the FBN group compared to that observed in the control and FB group. Additionally, a greater amount of spindle, elongated, and wavy shaped myofibroblasts was observed in the wound area of FBN group compared to observations in the other groups (Fig. 13).

8. Evaluation of micro-CT in calvarial defect rat model

Representative cross-sectional images and data analyses of each groups at 4 and 8 weeks after surgery are shown in Fig. 14. BV and BV/TV were measured. Additionally, bone healing parameters were analyzed for Tb Th, Tb N, and Tb Sp. At 4 and 8 weeks after surgery, the values for BV, BV/TV, Tb Th, Tb N, and Tb Sp for each group

are shown in Table 3 and Figs. 15−17.

For sponge experiments, BV, BV/TV, and bone healing parameters were highest in the 0.01 mM FBN group at 4 and 8 weeks after the surgery. There were also statistically significant differences between controls and the 0.01 mM FBN, 0.05 mM FB, and 0.01 mM FBN groups at 4 weeks after the surgery in regard to BV; between controls and the 0.01 mM FBN, 0.05 mM FB, and 0.01 mM FBN groups at 8 weeks after the surgery in regard to BV; between controls and the 0.01 mM FBN, 0.05 mM FB, and 0.01 mM FBN groups at 4 weeks after the surgery in regard to BV/TV; between controls and the 0.01 mM FBN, 0.05 mM FB, and 0.05 mM FBN groups, the 0.05 mM FB and 0.01 mM FBN groups, and the 0.05 mM FBN and 0.01 mM FBN groups at 8 weeks after the surgery in regard to BV/TV; between the 0.05 mM FB and 0.01 mM FBN groups at 8 weeks after the surgery in regard to Tb N, between the 0.05 mM FB and 0.01 mM FBN groups at 4 weeks after the surgery in regard to Tb Se; and between the 0.05 mM FB and 0.01 mM FBN groups at 8 weeks after the surgery in regard to Tb Sp ($p < 0.05$).

For bone particle experiments, BV, BV/TV, and bone healing parameters were highest in the 0.01 mM FBN group at 4 and 8 weeks

after the surgery, although there were no statistically significant differences. Additionally, bone healing parameters were highest in the 0.01 mM FBN group at 4 and 8 weeks after the surgery. There were statistically significant differences between controls and the 0.05 mM FB group and controls and the 0.05 mM FBN at 4 weeks after the surgery in regard to Tb Th; between controls and the 0.01 mM FBN, 0.05 mM FB, and 0.01 mM FBN groups at 8 weeks after the surgery in regard to Tb Th; between the 0.05 mM FB group and the 0.01 mM FBN group at 4 weeks after the surgery in regard to Tb Sp; and between the 0.05 mM FB group and the 0.01 mM FBN group at 8 weeks after the surgery in regard to Tb Sp ($p < 0.05$).

9. Histology for evaluation of bone formation in calvarial defect rat model

Representative histological images for each group at 4 and 8 weeks after surgery are shown in Fig. 18. For bone particle experiments, the average BV/TV values of control, 0.05 mM FB, 0.05 mM FB, and 0.01 mM FBN groups at 4 and 8 weeks after the surgery were 38.34 ± 4.24%, 38.02 ± 3.46%, 42.89 ± 3.35%, 43.52 ± 3.054% at 4

weeks after the surgery and 42.93 ± 3.55%, 43.32 ± 3.31%, 47.40 ± 2.73%, 48.06 ± 3.54% at 8 weeks after the surgery, respectively. BV/TV values were highest in the 0.01 mM FBN group at 4 and 8 weeks after the surgery. There were statistically significant differences between controls and the 0.05 mM FBN group, controls and the 0.01 mM FBN, 0.05 mM FB and 0.05 mM FBN groups, and the 0.05 mM FB group and the 0.01 mM FBN group at 4 and 8 weeks after the surgery ($p < 0.05$). In collagen sponge experiments, the average values of the control, 0.05 mM FB, 0.05 mM FB, and 0.01 mM FBN groups at 4 and 8 weeks after the surgery were 59.84 ± 5.82%, 59.42 ± 7.08%, 62.76 ± 6.34%, and 69.86 ± 6.16% at 4 weeks and 69.56 ± 4.25%, 69.53 ± 6.14%, 73.16 ± 4.18%, and 78.96 ± 4.23% at 8 weeks after the surgery, respectively. BV/TV values were highest in the 0.01 mM FBN group at 4 and 8 weeks after the surgery. There were statistically significant differences between the controls and the 0.01 mM FBN, 0.05 mM FB, and 0.01 mM FBN groups at 4 weeks after the surgery and between the controls and the 0.01 mM FBN, 0.05 mM FB, and 0.01 mM FBN groups and the 0.05 mM FBN and 0.01 mM FBN groups at 8 weeks after the surgery ($p < 0.05$). The results of histological analysis for BV/TV were

consistent with those of micro-CT analyses in the collagen sponge group. In the 0.01 mM FBN group treated with bone particles and sponges, bone density was significantly higher than that of the control group at 4 and 8 weeks after surgery

For CD31-staining, the microvessel density is shown in Table 4. MVD was highest in the FBN group treated with collagen sponges compared to that of the control group at 4 weeks after surgery. The MVD at 8 weeks after surgery was lower than the MVD at 4 weeks after surgery. For the bone particle experiment, CD31 was not abundantly detected in any of the groups (Fig. 19).

V. Discussion

This study examined the effects of a NO-releasing compound in the context of biocompatibility, soft tissue healing, and hard tissue bone formation. Several NO donors have been developed to allow for exogenous delivery of NO. Among these NO donors, NONOates produce two NO molecules. Materials that possess secondary amines can be easily functionalized into NONOates. FB is a biodegradable compound that possesses macromolecular structure. The compound becomes a liquid at low temperatures and gels at body temperature[72]. After pluronic F68 and BPEI are conjugated, NONOates are functionalized to the secondary amine of BPEI. Pluronic F68 is highly hydrophilic and is a constituent of the NO donors to which various substances can be conjugated[73]. NONOates act as a source of NO, and pluronic F68 acts as a depot for NO release. FBN contains a low percentage of BPEI that can cause cytotoxicity; however, BPEI contains large amounts of NONOates. The positive charge of FB (20 mv) can cause the cell wall to break by interacting with the negatively charged cell wall in bacteria[74]. Based on this, FB does exhibit some cytotoxicity. However, when NONOates are attached, the positive charge of FB decreases so that the surface charge of FBN is close to

zero. Compared to that of FB, the cytotoxicity of FBN is reduced, and the antibacterial effect is increased. It has also been reported that macromolecular NO donors such as FBN exhibit higher antimicrobial activity than do small molecule NO donors[75]. The total amount of NO released is more important than the instantaneous NO concentration in regard to the bactericidal effect[76,77]. Higher instantaneous NO concentrations cause an increase in cytotoxicity[78]. The duration of NO release is also an important factor in regard to the antimicrobial effect. Thus, lower instantaneous NO concentrations and a longer duration of NO release make more advantageous as NO donors. Previously, NO release was measured using the Griess assay[79]; however, in this study, NO was measured using a real time chemiluminescence NO analyzer. NO released from FBN was measured, and the amount of NO released was 117.5 nmol for 8.03 hours. The release half-life of NO was 53.1 minutes. The maximum instantaneous NO concentration was 117.5 pmol, and this was higher than that for the system described previously[80].

Pluronic F68 does not exhibit antimicrobial effects. FB exerted an insufficient bactericidal effect, indicating that the positive charge of FB is not sufficient to destroy the bacterial cell membrane. The MBC

of FBN against *P. gingivalis* was 1 mM. This indicates that the role of NO in antimicrobial activity is important. The antibacterial effect of NO is due to the substances produced by the reaction between NO radicals and peroxides[81]. Peroxynitrite ($ONOO^-$) produced by the reaction between NO and peroxide results in the peroxidization of lipids and breaks down DNA strands, ultimately causing antibacterial activity. The bacterial membranes are destroyed, and DNA is damaged. Using SEM, membrane breakdown was observed in bacteria treated with FBN (Fig. 6).

Therapeutic agents used in the clinic should not cause side effects or cytotoxicity[82]. The positive charge on the surface and the rapidly released NO can damage cells, and it is therefore necessary to evaluate cytotoxicity. To accomplish this, we evaluated the viability of HGF-1 cells after treatment with FB and FBN. HGF-1 cells were used to evaluate the potential for use as a therapeutic agent within the oral cavity. After HGF-1 cells were treated with FB and FBN for 24 hours, MTT assays were performed. The cell viability in response to FBN and FB was 77.95 ± 2.08 % and 89.96 ± 1.84%, respectively. Low cell viability was observed in FB-treated cells due to the positive charge on the surface of FB. Additionally, HGF-1 cells

treated with FBN showed enhanced migratory ability in a scratch assay as measured by the covered area at 24 hours after scratching. Increased migration capacity can promote wound healing. Ulcers within the oral cavity are a common disease. For the treatment of such oral ulcers, NO can be used as a therapeutic agent owing to its ability to improve the migration of fibroblasts.

Wound healing occurs through the inflammatory, proliferative, and remodeling phases, and NO participates in each phase of wound healing. In the inflammatory phase, NO vasodilates blood vessels and inhibits platelet formation. In the proliferation phase, NO promotes re-epithelialization and angiogenesis. In the remodeling phase, NO promotes collagen formation[83-85]. NO has been studied as a therapeutic agent for wound healing. Masters *et al*. demonstrated the ability to accumulate more collagen through the use of NO in chronic inflammation[86]. Blecher *et al*. showed that wound healing was improved in immunosuppressed mice treated with NO[5]. Lowe *et al*. revealed that wound healing was improved through the use of bandages containing NO[87]. In this study, the wound healing rate was high, indicating that application of FBN as a donor of NO promoted wound healing on both day 7 and day 14. This is consistent with the

results of other studies[23,88,89]. These data indicate that FBN increases wound healing during the initial wound healing process. FB also promoted wound healing compared to that observed in the control group. Changing the FB to a gel form at body temperature likely contributed to this wound protection. The high molecular weight compound FB is helpful in the context of wound healing by protecting the wound. However, the addition of NO to FB showed higher healing ability than that of FB on both day 7 and 14.

To observe re-epithelialization, H&E staining was performed to determine the structure of the mucosa. On days 7 and 14, re-epithelialization was increased in the FBN group compared to that of the other groups. NO stimulates the proliferation of fibroblasts, endothelial cells, and keratinocytes involved in at the start of the proliferation phase[90-92]. Externally administered NO diffuses into the wound, and the effects described above can occur. CK-14 was used to assess the epithelialization of the oral epithelium and newly forming keratinocytes[88]. CK-14 expressed in basal keratinocytes, is resistant to mechanical stimuli, helps maintain epithelial cell shape, and is a regulator associated with terminal differentiation of keratinocytes[93]. There were no differences in staining intensity in all

groups; however, CK-14 was positive in most suprabasal keratinocytes in the FBN group on day 14. At this time, differentiation of keratinocytes and cell migration occurred, and re-epithelialization was almost completed.

In the early stages of wound healing, fibroblasts migrate to the wound site and are converted into myofibroblasts within 3-4 days[94]. The primary function of myofibroblasts is to facilitate the contraction of wounds by synthesizing laminin, thrombospondin, collagen types I-VI, proteoglycans, and glycoproteins. Myofibroblast levels are increased from the inflammatory stage to the proliferation stage. α-SMA from myofibroblasts regulates proteins associated with contraction[95]. Wound contraction can be assessed by observing α-SMA levels. On days 7 and 14, α-SMA was more widely observed in the FBN group compared to levels in the other groups, indicating that wound contraction was more active in the FBN group. This suggests that FBN initially increases the proliferation of myofibroblasts that are required for initial wound contraction.

Bone formation and absorption are important processes required for the maintenance of bone remodeling and the healing of the micro damage. NO has been investigated as an important regulator of this

bone formation and absorption function. Low concentrations of NO stimulated osteoblasts and inhibited bone resorption by osteoclasts. High concentrations of NO caused bone loss[96]. When mechanical stimulation was applied to bones, NO was produced and osteoblasts were stimulated[97]. NO synthase (NOS) that stimulates NO production includes a neuronal form (nNOS), an inducible form (iNOS), and an endothelial form (eNOS)[35,36]. Bone formation was reduced in eNOS-deficient mice[98], and bone resorption was activated in mice with iNOS activation. Inflammation caused by cytokines increased iNOS[99], and estrogen increased eNOS in osteoblasts[100]. Wimalawansa *et al.* measured the lumbar spine BMD and femur weight of ovariectomy rats in the estrogen and nitroglycerin groups. The estrogen and nitroglycerin groups exhibited higher measured values compared to those of the control group. It has been shown that nitroglycerin prevents bone loss caused by ovariectomy[40]. Sunil *et al.* revealed that in castrated rats, an increase in BMD by testosterone was blocked by administration of NOS blockers. This study suggested that NO therapy may improve bone loss in men with hypogonadism and in elderly men. It has been reported that NO therapy has many advantages over the use of estrogen replacement therapy in

menopausal women, selective estrogen receptor modulator (SERM), male testosterone, and selective androgen receptor modulator (SARM)[101]. Wimalawansa *et al.* demonstrated that estrogen and nitroglycerin (30 mg/day) administered to maintain BMD in oophorectomized women exhibited nearly the same efficacy. It was shown that urinary N-telopeptide (bone absorption) and serum osteocalcin (bone formation) remained at the same level in women treated with nitroglycerin and estrogen[102]. Armor *et al.* reported a decrease in BMD and cortical thinning in mice with eNOS deficiency compared to that in controls, and they showed that estrogen anabolic activity was reduced even when a high dose of exogenous estrogen was administered to mice with eNOS deficiency[103]. Rejnmark *et al.* reported that patients taking organic nitrates (nitroglycerin, isosorbide mononitrate, and isosorbide dinitrate) had a lower risk of fracture and a 15% reduction in hip fractures in a case-controlled study comparing 124,655 subjects with fractures[104]. So far, these studies have focused mainly on the identification of BMD by systemic administration of NO. The agents used for systemic administration were nitroglycerin and nitrate. Many studies have reported that nitroglycerin was administered to increase BMD in postmenopausal

women. Additionally, there are numerous *in vivo* studies comparing estrogen and nitroglycerin after ovariectomy. Systemic use of NO compounds such as nitroglycerin promoted bone formation. This study showed that local application of NO also promoted bone formation.

Angiogenesis is an important factor in wound healing and bone formation. NO exerts a mechanism of action that forms blood vessels[105,106]. Vascularization can be observed through the use of IHC on endothelial cells with CD31[107]. We observed that endothelial cells were present in proximity to new bone areas. At week 4, CD31-expressing endothelial cells were abundantly observed in the FBN group; however, the MVD at week 8 was lower than the MVD at week 4. It is likely that the microvessels were formed primarily during the early stage of bone formation, and the microvessels then decreased as the bone defect was mineralized. Based on this, it is likely that FBN induces angiogenesis during the early stage of bone formation. In the bone particle experiment, CD31 was not abundantly detected in any of the groups. NO cannot be delivered effectively to surrounding hard tissue in the bone particle group and the angiogenesis action of NO may be limited.

Several NO-releasing compounds have been studied to evaluate the effect of NO on wound healing. Lowe *et al.* showed that wound healing was improved by applying a bandage with acrylonitrile NO polymer[108]. Blecher *et al.* showed that wound healing was promoted in immunodeficient mouse models using NO-loaded nanoparticles[109]. Masters *et al.* used NO-polymer hydrogels to evaluate the healing of chronic wounds in *in vivo* experiments and showed increased collagen accumulation and granulation[110]. Kim *et al.* showed that re-epithelialization, angiogenesis, and collagen deposition were improved by applying FBN at the skin sites in rats[12]. To date, studies examining wound healing have been conducted on cutaneous wounds, and good results have been obtained. However, there are many oral mucosal diseases that occur repeatedly within the oral area. Treatments of mucosal diseases include decontamination with chlorohexidine, application of agents containing a local anesthetic, and application of corticosteroids with strong anti-inflammatory actions. However, these treatments are only used to relieve symptoms. When the steroid is repeatedly applied for a long period of time, side effects that include a thinning the mucosal epithelium may occur. Treatment of recurrent oral mucosal diseases requires

regeneration of the epithelium. This *in vivo* experiment showed that accelerated wound closure can be achieved by enhanced re-epithelialization using an NO-releasing compound. Additionally, although cytotoxicity of FB was observed in an *in vitro* experiment, the wound healing rate of FB was increased compared to that of the control. This is likely due to the ability of pluronic F68 to change into a gel form at body temperature, thus protecting the wound. Compared to FB, FBN was observed to have low cytotoxicity and promoted mucosal healing. FBN is a biodegradable and hydrophilic compound that possesses macromolecular structure. FBN produce two NO molecules. FBN becomes a liquid at low temperatures and gels at body temperature[72]. The maximum instantaneous NO concentration was higher than that for the system described previously[80]. When FBN is stored at −20℃, NO is released and can be stored for a long time. When FBN is mixed with water, NO is released, so application is convenient. As such, FBN has many advantages over other NO donors.

In the field of oral maxillofacial surgery, there are many diseases such as cysts, tumors, and osteomyelitis that would benefit from the controlled local formation of bone. Here, we tested the degree of

osteogenesis by applying the NO-releasing compound topically. The effect of NO on osteogenesis was evaluated in the group treated with collagen sponges and bone grafts. In the group with collagen sponges, the NO-releasing compound application group exhibited higher rates of bone formation than the control group; however, in the group with bone grafts, there was no statistical difference in osteogenesis between the NO-releasing compound applied group and the control group. It is thought that NO was not easily transmitted to the surrounding tissues due to the presence of bone particles. It is thought that FBN can be applied to bone defects such as cysts and medication-related osteonecrosis of the jaw that do not require bone grafts. Prior to clinical applications, further experiments are required to more thoroughly examine FBN.

VI. Conclusion

In this study, the effects of the FBN were evaluated using *in vitro* and *in vivo* experiments. In the *in vitro* study, FBN exerted a bactericidal effect on *P. gingivalis*, and HGF-1 cells treated with FBN possessed high migration rates and viability. High migration rates are thought to be helpful in the context of palatal wound regeneration.

In the palatal wound mouse model, palatal wounds treated with FBN were assessed at 7 days and 14 days after wound formation. When the FBN was applied in the palatal wound mouse model, the palatal wound regeneration was enhanced within the soft tissue defect. The re-epithelialization effect of FBN on palatal mucosa was observed using IHC.

In the calvarial rat model, calvarial defects treated with FBN in combination with collagen sponges and bone particles were assessed at 4 weeks and 8 weeks after bone defect formation. When the FBN and collagen sponges were applied together in the calvarial defect rat model, osteogenesis was promoted within the bone defects. The observed increase in CD31 in the FBN and collagen sponge group suggests an accelerated angiogenesis effect during the early healing

process. However, considering the small number of experimental groups, additional studies will be required.

This study suggests that FBN can be effective for the treatment of ulcerative palatal wounds based on its ability to accelerate re-epithelialization and migration. When FBN was applied in combination with a collagen sponge, it could promote osteogenesis in a calvarial defect rat model. FBN may be effective for the treatment of bone defects; however, further animal and clinical studies should be performed.

Reference

1. Marletta M, Tayeh M, Hevel J: Unraveling the biological significance of nitric oxide. BioFactors (Oxford, England) 1990;2:219-225.
2. Kim J, Saravanakumar G, Choi HW, Park D, Kim WJ: A platform for nitric oxide delivery. Journal of Materials Chemistry B 2014;2:341-356.
3. George Broughton I, Janis JE, Attinger CE: Wound healing: an overview. Plastic and reconstructive surgery 2006;117:1e-S-32e-S.
4. Smith PC, Martínez C, Martínez J, McCulloch CA: Role of fibroblast populations in periodontal wound healing and tissue remodeling. Frontiers in physiology 2019;10.
5. Fang FC: Perspectives series: host/pathogen interactions. Mechanisms of nitric oxide-related antimicrobial activity. The Journal of clinical investigation 1997;99:2818-2825.
6. Hetrick EM, Shin JH, Stasko NA, Johnson CB, Wespe DA, Holmuhamedov E, et al.: Bactericidal efficacy of nitric oxide-releasing silica nanoparticles. Acs Nano 2008;2:235-246.

7. Keefer LK, Nims RW, Davies KM, Wink DA. "NONOates" (1-substituted diazen-1-ium-1, 2-diolates) as nitric oxide donors: convenient nitric oxide dosage forms Methods in enzymology, Elsevier.1996:281-293.

8. Nakashima K, Anzai T, Fujimoto Y: Fluorescence studies on the properties of a Pluronic F68 micelle. Langmuir 1994;10:658-661.

9. Kwon JS, Park IK, Cho AS, Shin SM, Hong MH, Jeong SY, et al.: Enhanced angiogenesis mediated by vascular endothelial growth factor plasmid-loaded thermo-responsive amphiphilic polymer in a rat myocardial infarction model. Journal of Controlled Release 2009;138:168-176.

10. Namgung R, Nam S, Kim SK, Son S, Singha K, Kwon J-S, et al.: An acid-labile temperature-responsive sol-gel reversible polymer for enhanced gene delivery to the myocardium and skeletal muscle cells. Biomaterials 2009;30:5225-5233.

11. Kim J, Lee Y, Singha K, Kim HW, Shin JH, Jo S, et al.: NONOates-polyethylenimine hydrogel for controlled nitric oxide release and cell proliferation modulation. Bioconjugate chemistry 2011;22:1031-1038.

12. Kang Y, Kim J, Lee YM, Im S, Park H, Kim WJ: Nitric oxide-releasing polymer incorporated ointment for cutaneous wound healing. Journal of Controlled Release 2015;220:624-630.

13. Park J, Kim J, Singha K, Han D-K, Park H, Kim WJ: Nitric oxide integrated polyethylenimine-based tri-block copolymer for efficient antibacterial activity. Biomaterials 2013;34:8766-8775.

14. Stasko NA, Schoenfisch MH: Dendrimers as a scaffold for nitric oxide release. Journal of the American Chemical Society 2006;128:8265-8271.

15. Bielefeld KA, Amini-Nik S, Alman BA: Cutaneous wound healing: recruiting developmental pathways for regeneration. Cellular and Molecular Life Sciences 2013;70:2059-2081.

16. Eming SA, Martin P, Tomic-Canic M: Wound repair and regeneration: mechanisms, signaling, and translation. Science translational medicine 2014;6:265sr266-265sr266.

17. Politis C, Schoenaers J, Jacobs R, Agbaje JO: Wound healing problems in the mouth. Frontiers in physiology 2016;7:507.

18. Cohen IK, Die-gelmann RF, Lindblad WJ, Hugo NE: Wound healing: biochemical and clinical aspects. Plastic and

Reconstructive Surgery 1992;90:926.

19. Gonzalez ACdO, Costa TF, Andrade ZdA, Medrado ARAP: Wound healing—A literature review. Anais brasileiros de dermatologia 2016;91:614—620.

20. Kirsner RS, Eaglstein WH: The wound healing process. Dermatologic clinics 1993;11:629—640.

21. Hunt TK, Hopf HW: Wound healing and wound infection: what surgeons and anesthesiologists can do. Surgical Clinics of North America 1997;77:587—606.

22. Seymour RA, Meechan JG, Yates MS, Seymour RA, Walton JG. Pharmacology and dental therapeutics. Oxford University Press Oxford:,1999.

23. George Broughton I, Janis JE, Attinger CE: The basic science of wound healing. Plastic and reconstructive surgery 2006;117:12S—34S.

24. Brandi ML, Hukkanen M, Umeda T, Moradi—Bidhendi N, Bianchi S, Gross SS, et al.: Bidirectional regulation of osteoclast function by nitric oxide synthase isoforms. Proceedings of the National Academy of Sciences 1995;92:2954—2958.

25. Wimalawansa SJ: Rationale for using nitric oxide donor therapy for prevention of bone loss and treatment of osteoporosis in humans. Annals of the New York Academy of Sciences 2007;1117:283-297.

26. Wimalawansa SJ: Nitric oxide: new evidence for novel therapeutic indications. Expert opinion on pharmacotherapy 2008;9:1935-1954.

27. Shikano K, Ohlstein EH, Berkowitz BA: Differential selectivity of endothelium-derived relaxing factor and nitric oxide in smooth muscle. British journal of pharmacology 1987;92:483-485.

28. Ignarro LJ, Buga GM, Wood KS, Byrns RE, Chaudhuri G: Endothelium-derived relaxing factor produced and released from artery and vein is nitric oxide. Proceedings of the National Academy of Sciences 1987;84:9265-9269.

29. Arnold WP, Mittal CK, Katsuki S, Murad F: Nitric oxide activates guanylate cyclase and increases guanosine 3′ : 5′ -cyclic monophosphate levels in various tissue preparations. Proceedings of the National Academy of Sciences 1977;74:3203-3207.

30. SoRelle R: Nobel prize awarded to scientists for nitric oxide discoveries. Circulation 1998;98:2365-2366.

31. Carpenter AW, Schoenfisch MH: Nitric oxide release: Part II. Therapeutic applications. Chemical Society Reviews 2012;41:3742-3752.

32. Jen MC, Serrano MC, Van Lith R, Ameer GA: Polymer-based nitric oxide therapies: Recent insights for biomedical applications. Advanced functional materials 2012;22:239-260.

33. Naghavi N, de Mel A, Alavijeh OS, Cousins BG, Seifalian AM: Nitric oxide donors for cardiovascular implant applications. Small 2013;9:22-35.

34. Fukumura D, Kashiwagi S, Jain RK: The role of nitric oxide in tumour progression. Nature Reviews Cancer 2006;6:521-534.

35. Pollock JS, Förstermann U, Mitchell JA, Warner TD, Schmidt H, Nakane M, et al.: Purification and characterization of particulate endothelium-derived relaxing factor synthase from cultured and native bovine aortic endothelial cells. Proceedings of the National Academy of Sciences 1991;88:10480-10484.

36. Xie Q-w, Cho HJ, Calaycay J, Mumford RA, Swiderek KM, Lee

TD, et al.: Cloning and characterization of inducible nitric oxide synthase from mouse macrophages. Science 1992;256:225-228.

37. Schäffer MR, Tantry U, Gross SS, Wasserkrug HL, Barbul A: Nitric oxide regulates wound healing. Journal of surgical research 1996;63:237-240.

38. Witte M, Kiyama T, Barbul A: Nitric oxide enhances experimental wound healing in diabetes. British journal of surgery 2002;89:1594-1601.

39. Wimalawansa SJ: Nitric oxide: novel therapy for osteoporosis. Expert opinion on pharmacotherapy 2008;9:3025-3044.

40. Wimalawansa S, De Marco G, Gangula P, Yallampalli C: Nitric oxide donor alleviates ovariectomy-induced bone loss. Bone 1996;18:301-304.

41. Mocellin S, Bronte V, Nitti D: Nitric oxide, a double edged sword in cancer biology: searching for therapeutic opportunities. Medicinal research reviews 2007;27:317-352.

42. Al-Sa'Doni H, Ferro A: S-Nitrosothiols: a class of nitric oxide-donor drugs. Clinical science 2000;98:507-520.

43. Yamamoto T, Bing RJ: Nitric Oxide Donors (44565).

Proceedings of the Society for Experimental Biology and Medicine 2000;225:200-206.

44. Hrabie JA, Keefer LK: Chemistry of the nitric oxide-releasing diazeniumdiolate ("nitrosohydroxylamine") functional group and its oxygen-substituted derivatives. Chemical reviews 2002;102:1135-1154.

45. Sciubba JJ, Waterhouse JP, Meyer J: A fine structural comparison of the healing of incisional wounds of mucosa and skin. Journal of Oral Pathology & Medicine 1978;7:214-227.

46. Walsh L, L'Estrange P, Seymour G: High magnification in situ viewing of wound healing in oral mucosa. Australian dental journal 1996;41:75-79.

47. Harrison JW, Jurosky KA: Wound healing in the tissues of the periodontium following periradicular surgery. III. The osseous excisional wound. Journal of endodontics 1992;18:76-81.

48. Enoch S, Moseley R, Stephens P, Thomas DW: The oral mucosa: a model of wound healing with reduced scarring. Oral Surgery 2008;1:11-21.

49. Theoret CL: The pathophysiology of wound repair. Veterinary Clinics: Equine Practice 2005;21:1-13.

50. Campisi J. The role of cellular senescence in skin aging Journal of Investigative Dermatology Symposium Proceedings, Elsevier.1998:1-5.

51. Liu J, Bian Z, Kuijpers-Jagtman A, Von den Hoff J: Skin and oral mucosa equivalents: construction and performance. Orthodontics & craniofacial research 2010;13:11-20.

52. Squier CA, Kremer MJ: Biology of oral mucosa and esophagus. JNCI Monographs 2001;2001:7-15.

53. Hsieh PC, Jin YT, Chang CW, Huang CC, Liao SC, Yuan K: Elastin in oral connective tissue modulates the keratinization of overlying epithelium. Journal of clinical periodontology 2010;37:705-711.

54. Wong JW, Gallant-Behm C, Wiebe C, Mak K, Hart DA, Larjava H, et al.: Wound healing in oral mucosa results in reduced scar formation as compared with skin: evidence from the red Duroc pig model and humans. Wound Repair and Regeneration 2009;17:717-729.

55. Li J, Ireland GW, Farthing PM, Thornhill MH: Epidermal and oral keratinocytes are induced to produce RANTES and IL-8 by cytokine stimulation. Journal of investigative dermatology

1996;106:661-666.

56. Stavenuiter A, Schilte M, Ter Wee P, Beelen R: Angiogenesis in peritoneal dialysis. Kidney and Blood Pressure Research 2011;34:245-252.

57. Mak K, Manji A, Gallant-Behm C, Wiebe C, Hart DA, Larjava H, et al.: Scarless healing of oral mucosa is characterized by faster resolution of inflammation and control of myofibroblast action compared to skin wounds in the red Duroc pig model. Journal of dermatological science 2009;56:168-180.

58. Szpaderska A, Walsh C, Steinberg M, DiPietro L: Distinct patterns of angiogenesis in oral and skin wounds. Journal of dental research 2005;84:309-314.

59. Ricard-Blum S: The collagen family. Cold Spring Harbor perspectives in biology 2011;3:a004978.

60. Schrementi ME, Ferreira AM, Zender C, DiPietro LA: Site-specific production of TGF-β in oral mucosal and cutaneous wounds. Wound Repair and Regeneration 2008;16:80-86.

61. Schenk RK, Buser D, Hardwick WR, Dahlin C: Healing pattern of bone regeneration in membrane-protected defects: a histologic study in the canine mandible. International journal of

oral & maxillofacial implants 1994;9.

62. Javed A, Chen H, Ghori FY: Genetic and transcriptional control of bone formation. Oral and Maxillofacial Surgery Clinics 2010;22:283–293.

63. Buser D: years of Guided Bone Regeneration (Decision criteria for a Simultaneous GBR procedure). Chicago Quintessence Books;2009:123–152.

64. Giannoudis PV, Dinopoulos H, Tsiridis E: Bone substitutes: an update. Injury 2005;36:S20–S27.

65. James AW, LaChaud G, Shen J, Asatrian G, Nguyen V, Zhang X, et al.: A review of the clinical side effects of bone morphogenetic protein-2. Tissue Engineering Part B: Reviews 2016;22:284–297.

66. Turner N, Grose R: Fibroblast growth factor signalling: from development to cancer. Nature Reviews Cancer 2010;10:116–129.

67. Weller R: Nitric oxide: a key mediator in cutaneous physiology. Clinical and Experimental Dermatology: Clinical Dermatology 2003;28:511–514.

68. Adamskaya N, Dungel P, Mittermayr R, Hartinger J,

Feichtinger G, Wassermann K, et al.: Light therapy by blue LED improves wound healing in an excision model in rats. Injury 2011;42:917-921.

69. Rakhmatia YD, Ayukawa Y, Furuhashi A, Koyano K: Microcomputed tomographic and histomorphometric analyses of novel titanium mesh membranes for guided bone regeneration: a study in rat calvarial defects. International Journal of Oral & Maxillofacial Implants 2014;29.

70. Goscinski MA, Suo ZH, Nesland JM, Florenes VA, GIERCKSKY KE: Dipeptidyl peptidase IV expression in cancer and stromal cells of human esophageal squamous cell carcinomas, adenocarcinomas and squamous cell carcinoma cell lines. Apmis 2008;116:823-831.

71. Weidner N, Semple JP, Welch WR, Folkman J: Tumor angiogenesis and metastasis—correlation in invasive breast carcinoma. New England Journal of Medicine 1991;324:1-8.

72. Zhou Z, Annich GM, Wu Y, Meyerhoff ME: Water-soluble poly (ethylenimine)-based nitric oxide donors: preparation, characterization, and potential application in hemodialysis. Biomacromolecules 2006;7:2565-2574.

73. Kuo JHS: Effect of Pluronic-block copolymers on the reduction of serum-mediated inhibition of gene transfer of polyethyleneimine–DNA complexes. Biotechnology and applied Biochemistry 2003;37:267–271.

74. Azevedo M, Ramalho P, Silva A, Teixeira–Santos R, Pina–Vaz C, Rodrigues A: Polyethyleneimine and polyethyleneimine–based nanoparticles: novel bacterial and yeast biofilm inhibitors. Journal of medical microbiology 2014;63:1167–1173.

75. Backlund CJ, Worley BV, Schoenfisch MH: Anti–biofilm action of nitric oxide–releasing alkyl–modified poly (amidoamine) dendrimers against Streptococcus mutans. Acta biomaterialia 2016;29:198–205.

76. Backlund C, Sergesketter A, Offenbacher S, Schoenfisch M: Antibacterial efficacy of exogenous nitric oxide on periodontal pathogens. Journal of dental research 2014;93:1089–1094.

77. Backlund C, Worley B, Sergesketter A, Schoenfisch M: Kinetic–dependent killing of oral pathogens with nitric oxide. Journal of dental research 2015;94:1092–1098.

78. Al–Ani B, Hewett PW, Ahmed S, Cudmore M, Fujisawa T,

Ahmad S, et al.: The release of nitric oxide from S-nitrosothiols promotes angiogenesis. PLoS One 2006;1:e25.

79. Wink DA, Kasprzak KS, Maragos CM, Elespuru RK, Misra M, Dunams TM, et al.: DNA deaminating ability and genotoxicity of nitric oxide and its progenitors. Science 1991;254:1001-1003.

80. Charville GW, Hetrick EM, Geer CB, Schoenfisch MH: Reduced bacterial adhesion to fibrinogen-coated substrates via nitric oxide release. Biomaterials 2008;29:4039-4044.

81. Brunelli L, Crow JP, Beckman JS: The comparative toxicity of nitric oxide and peroxynitrite to Escherichia coli. Archives of biochemistry and biophysics 1995;316:327-334.

82. Williams DF: On the mechanisms of biocompatibility. Biomaterials 2008;29:2941-2953.

83. Sande L, Sanchez M, Montes J, Wolf AJ, Morgan MA, Omri A, et al.: Liposomal encapsulation of vancomycin improves killing of methicillin-resistant Staphylococcus aureus in a murine infection model. Journal of Antimicrobial Chemotherapy 2012;67:2191-2194.

84. Ivanov IE, Morrison AE, Cobb JE, Fahey CA, Camesano TA:

Creating antibacterial surfaces with the peptide chrysophsin-1. ACS applied materials & interfaces 2012;4:5891-5897.

85. Mancinelli RL, McKAY CP: Effects of nitric oxide and nitrogen dioxide on bacterial growth. Appl Environ Microbiol 1983;46:198-202.

86. Hardwick J, Tucker A, Wilks M, Johnston A, Benjamin N: A novel method for the delivery of nitric oxide therapy to the skin of human subjects using a semi-permeable membrane. Clinical Science 2001;100:395-400.

87. Jones ML, Ganopolsky JG, Labbé A, Wahl C, Prakash S: Antimicrobial properties of nitric oxide and its application in antimicrobial formulations and medical devices. Applied microbiology and biotechnology 2010;88:401-407.

88. Braiman-Wiksman L, Solomonik I, Spira R, Tennenbaum T: Novel insights into wound healing sequence of events. Toxicologic pathology 2007;35:767-779.

89. Dreifke MB, Jayasuriya AA, Jayasuriya AC: Current wound healing procedures and potential care. Materials Science and Engineering: C 2015;48:651-662.

90. Heck DE, Laskin DL, Gardner CR, Laskin JD: Epidermal growth

factor suppresses nitric oxide and hydrogen peroxide production by keratinocytes. Potential role for nitric oxide in the regulation of wound healing. Journal of Biological Chemistry 1992;267:21277-21280.

91. Krischel V, Bruch-Gerharz D, Suschek C, Kröncke K-D, Ruzicka T, Kolb-Bachofen V: Biphasic effect of exogenous nitric oxide on proliferation and differentiation in skin derived keratinocytes but not fibroblasts. Journal of Investigative Dermatology 1998;111:286-291.

92. Ziche M, Morbidelli L, Masini E, Granger H, Geppetti P, Ledda F: Nitric oxide promotes DNA synthesis and cyclic GMP formation in endothelial cells from postcapillary venules. Biochemical and biophysical research communications 1993;192:1198-1203.

93. Alam H, Sehgal L, Kundu ST, Dalal SN, Vaidya MM: Novel function of keratins 5 and 14 in proliferation and differentiation of stratified epithelial cells. Molecular biology of the cell 2011;22:4068-4078.

94. Klingberg F, Hinz B, White ES: The myofibroblast matrix: implications for tissue repair and fibrosis. The Journal of

pathology 2013;229:298-309.

95. Hinz B, Celetta G, Tomasek JJ, Gabbiani G, Chaponnier C: Alpha-smooth muscle actin expression upregulates fibroblast contractile activity. Molecular biology of the cell 2001;12:2730-2741.

96. Wimalawansa SJ. Calcitonin: History, Physiology, Pathophysiology and Therapeutic Applications Osteoporosis in Men, Elsevier.2010:653-666.

97. Turner CH, Takano Y, Owan I, Murrell G: Nitric oxide inhibitor L-NAME suppresses mechanically induced bone formation in rats. American Journal of Physiology-Endocrinology and Metabolism 1996;270:E634-E639.

98. Aguirre J, Buttery L, O'Shaughnessy M, Afzal F, de Marticorena IF, Hukkanen M, et al.: Endothelial nitric oxide synthase gene-deficient mice demonstrate marked retardation in postnatal bone formation, reduced bone volume, and defects in osteoblast maturation and activity. The American journal of pathology 2001;158:247-257.

99. Armour KE, Van'T Hof RJ, Grabowski PS, Reid DM, Ralston SH: Evidence for a pathogenic role of nitric oxide in

inflammation-induced osteoporosis. Journal of Bone and Mineral Research 1999;14:2137-2142.

100. Armour KE, Ralston SH: Estrogen upregulates endothelial constitutive nitric oxide synthase expression in human osteoblast-like cells. Endocrinology 1998;139:799-802.

101. Wimalawansa SJ: Nitric oxide and bone. Annals of the New York Academy of Sciences 2010;1192:391.

102. Wimalawansa SJ: Nitroglycerin therapy is as efficacious as standard estrogen replacement therapy (Premarin) in prevention of oophorectomy-induced bone loss: a human pilot clinical study. Journal of Bone and Mineral Research 2000;15:2240-2244.

103. Armour KE, Armour KJ, Gallagher ME, Go decke A, Helfrich MH, Reid DM, et al.: Defective bone formation and anabolic response to exogenous estrogen in mice with targeted disruption of endothelial nitric oxide synthase. Endocrinology 2001;142:760-766.

104. Rejnmark L, Vestergaard P, Mosekilde L: Decreased fracture risk in users of organic nitrates: a nationwide case-control study. Journal of Bone and Mineral Research 2006;21:1811-

1817.

105. Ziche M, Morbidelli L: Nitric oxide and angiogenesis. Journal of neuro-oncology 2000;50:139-148.

106. Liekens S, De Clercq E, Neyts J: Angiogenesis: regulators and clinical applications. Biochemical pharmacology 2001;61:253-270.

107. Pusztaszeri MP, Seelentag W, Bosman FT: Immunohistochemical expression of endothelial markers CD31, CD34, von Willebrand factor, and Fli-1 in normal human tissues. Journal of Histochemistry & Cytochemistry 2006;54:385-395.

108. Lowe A, Bills J, Verma R, Lavery L, Davis K, Balkus Jr K: Electrospun nitric oxide releasing bandage with enhanced wound healing. Acta biomaterialia 2015;13:121-130.

109. Han G, Nguyen LN, Macherla C, Chi Y, Friedman JM, Nosanchuk JD, et al.: Nitric oxide–releasing nanoparticles accelerate wound healing by promoting fibroblast migration and collagen deposition. The American journal of pathology 2012;180:1465-1473.

110. Masters KSB, Leibovich SJ, Belem P, West JL, Poole-Warren

LA: Effects of nitric oxide releasing poly (vinyl alcohol) hydrogel dressings on dermal wound healing in diabetic mice. Wound Repair and regeneration 2002;10:286-294.

Tables

Table 1. Condition of the immuohistochemistry (IHC).

Antigen	Primary antibodies				Antigen retrieval buffer	Detection method
	Clone	Origin	Incubation time (min)	Dilution		
CK-14	LL002	Novocastra,NC, UK	20	1:400	Tris-EDTA	HRP (Ventana kit)
α-SMA	1A4	NeoMarkers, CA, US	20	1:800	Tris-EDTA	HRP (Ventana kit)
CD-31	MEC 7.46	Abcam, CB, UK	20	1:200	Tris-EDTA	HRP (Ventana kit)

Abbreviation: CK-14: cytokeratin-14, α-SMA: α-smooth muscle actin, CD-31: cluster of differentiation-31, HRP: horseradish peroxidase-polymer, Tris-EDTA: Tris-ethylenediaminetetraacetic acid

Table 2. NO release properties of pluronic F68-branced polyethylenimine-NONOates (FBN).

$[NO]_t$[a]	$[NO]_m$[b]	t_m[c]	$t_{1/2}$[d]	t_d[e]
415	117.5	11.2	53.1	8.03

[a][NO]t, The total number of nanomoles (nmol/mg).

[b][NO]m, maximum instantaneous concentration (pmol/mg).

[c]tm, time required to reach [NO]m (min).

[d]t1/2, half-life (min).

[e]td, duration (h).

Table 3. Bone volume (BV, mm^3), bone volume fraction (BV/TV, %), number of trabeculae (Tb N, N/mm), trabecular separation (Tb Sp, mm), and trabecular thickness (Tb Th, mm) in control, 0.05 mM FB, 0.05 mM FBN, and 0.01 mM FBN with collagen sponge (A) and bone particle (B).

A

		Control	0.05 FB	0.05 FBN	0.01 FBN
BV (mm^3)	4W	2.120 ± 0.255*	2.113 ± 0.238*	2.309 ± 0.126	2.494 ± 0.173*†
	8W	2.421 ± 0.161*	2.379 ± 0.213*	2.598 ± 0.114	2.789 ± 0.124*†
BV/TV (%)	4W	62.260 ± 7.493*	62.070 ± 6.999*	67.808 ± 3.712	73.246 ± 5.103*†
	8W	71.079 ± 4.722*	69.860 ± 6.260†*	76.296 ± 3.350†*	81.91 ± 3.640*††
Tb Th (mm)	4W	0.103 ± 0.010	0.102 ± 0.009	0.105 ± 0.008	0.108 ± 0.004
	8W	0.116 ± 0.002	0.114 ± 0.003	0.115 ± 0.001	0.116 ± 0.001
Tb N (N/mm)	4W	6.101 ± 0.408	6.038 ± 0.394	6.206 ± 0.733	6.207 ± 0.724
	8W	6.538 ± 0.398	6.594 ± 0.423*	6.864 ± 0.489	7.384 ± 0.451†
Tb Sp (mm)	4W	0.107 ± 0.007	0.109 ± 0.008*	0.104 ± 0.006	0.099 ± 0.007†
	8W	0.097 ± 0.005	0.100 ± 0.007*	0.095 ± 0.007	0.089 ± 0.009†

The data is presented as mean ± standard deviation (SD). Abbreviation: 4W: four weeks after surgery, 8W: eight weeks after surgery, TV: tissue volume, BV: bone volume, BV/TV: bone volume/tissue volume, Tb Th: trabecular thickness, Tb N: trabecular number, Tb Sp: trabecular seperation, FB: pluronic F68−branced polyethylenimine, FBN: pluronic F68−branced polyethylenimine−NONOates, *: $p < 0.05$ vs. Control group, †: $p < 0.05$ vs. 0.05mM FB group, ‡: $p < 0.05$ vs. 0.05 mM FBN group, ※: $p < 0.05$ vs. 0.01 mM FBN group

B

		Control	0.05 FB	0.05 FBN	0.01 FBN
BV (mm^3)	4W	1.476 ± 0.139	1.468 ± 0.197	1.616 ± 0.143	1.644 ± 0.142
	8W	1.600 ± 0.143	1.597 ± 0.149	1.736 ± 0.139	1.759 ± 0.146
BV/TV (%)	4W	43.350 ± 4.100	43.113 ± 5.780	47.466 ± 4.204	48.277 ± 4.178
	8W	46.987 ± 4.187	46.911 ± 4.396	50.979 ± 4.084	51.656 ± 4.302
Tb Th (mm)	4W	0.105 ± 0.003†‡	0.103 ± 0.002*	0.105 ± 0.01*	0.106 ± 0.002
	8W	0.108 ± 0.003	0.107 ± 0.003	0.111 ± 0.002	0.111 ± 0.002
Tb N (N/mm)	4W	5.771 ± 0.449	5.422 ± 0.550	5.749 ± 0.299	6.312 ± 0.458
	8W	5.811 ± 0.549※	5.711 ± 0.615※	6.27 ± 0.36	6.544 ± 0.08*†
Tb Sp (mm)	4W	0.104 ± 0.007	0.109 ± 0.005※	0.1004 ± 0.004	0.099 ± 0.005†
	8W	0.094 ± 0.004	0.099 ± 0.004※	0.095 ± 0.004	0.091 ± 0.005†

The data is presented as mean ± standard deviation (SD). Abbreviation: 4W: four weeks after surgery, 8W: eight weeks after surgery, TV: tissue volume, BV: bone volume, BV/TV: bone volume/tissue volume, Tb Th: trabecular thickness, Tb N: trabecular number, Tb Sp: trabecular seperation, FB: pluronic F68-branced polyethylenimine, FBN: pluronic F68-branced polyethylenimine-NONOates, *: $p < 0.05$ vs. Control group, †: $p < 0.05$ vs. 0.05mM FB group, ‡: $p < 0.05$ vs. 0.05 mM FBN group, ※: $p < 0.05$ vs. 0.01 mM FBN group

Table 4. MVD (microvessel/mm^2) in control, 0.05 mM FB, 0.05 mM FBN and 0.01 mM FBN with collagen sponge and bone particle on weeks 4 and 8.

		Control	0.05 FB	0.05 FBN	0.01 FBN
Collagen experiment	4W	91	105	86	163
	8W	63	95	72	127
Bone particle experiment	4W	45	36	31	50
	8W	31	50	36	36

Abbreviation: 4W: four weeks after surgery, 8W: eight weeks after surgery, FB: pluronic F68-branced polyethylenimine, FBN: pluronic F68-branced polyethylenimine-NONOates

Figure legends and Figures

Figure 1. Macromolecule NO-releasing compound.

F68-BPEI

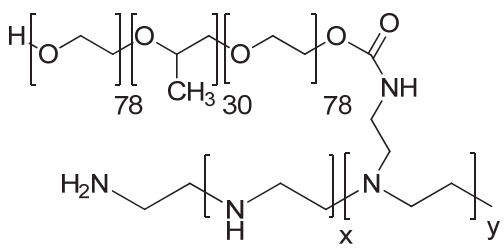

F68-BPEI-NONOates

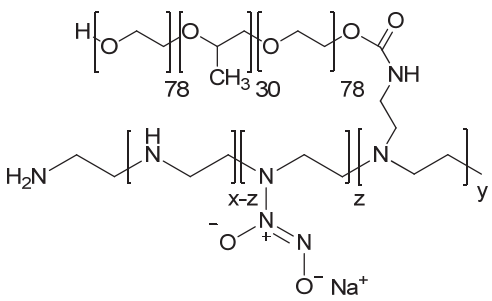

Figure 2. The time tables. (A) The soft tissue regeneration experiment of palatal wound model in BALB/C mouse, (B) The osteogenesis experiment of calvarial defect model in sprague-dawley rat.

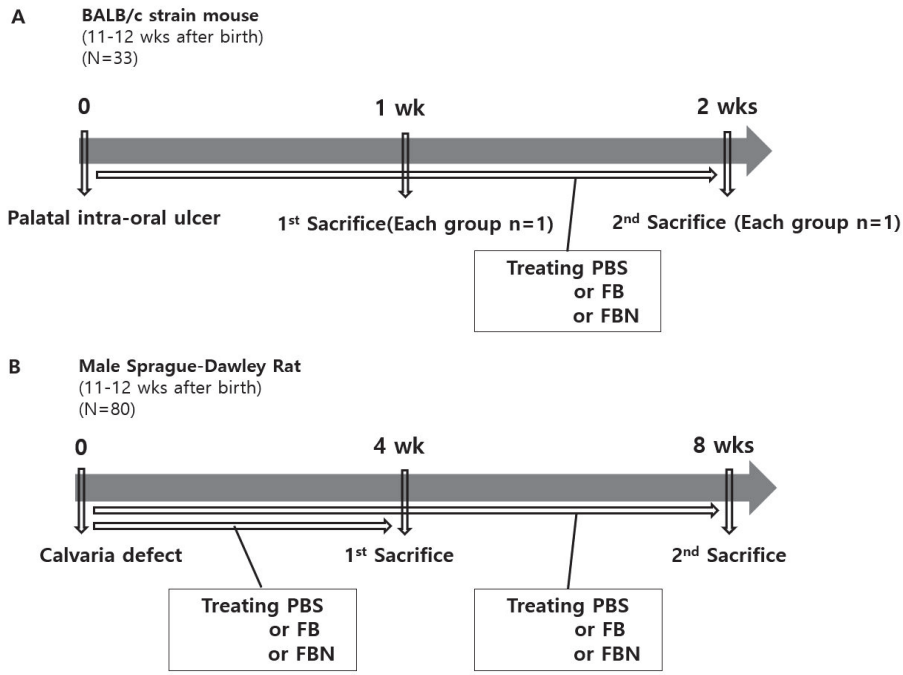

Figure 3. Calvarial defect formation. (A) Full-thickness calvarial defects on the Both sides, (B) Collagen sponge with PBS, 0.05 mM FB, 0.05 mM FBN, 0.01 mM FBN was filled in the Both sides, (C) Bone particles with PBS, 0.05 mM FB, 0.05 mM FBN, 0.01 mM FBN was filled in the Both sides.

Figure 4. NO releasing property of FBN. (A) NO concentration over time, (B) The cumulative NO release.

A

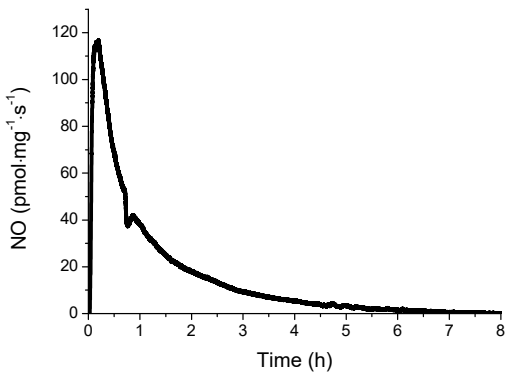

B

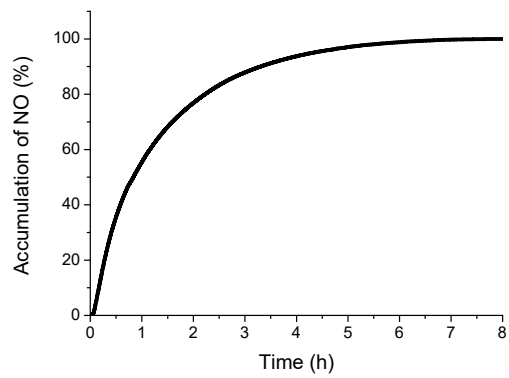

Figure 5. Bactericidal efficacy of NO-releasing compound.

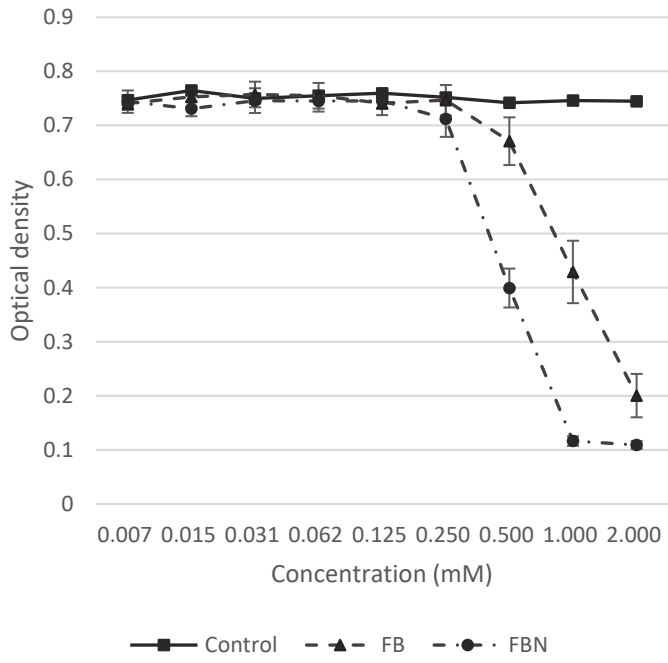

Figure 6. SEM image of *P. gingivalis*. (A) Treated with Dulbecco's phosphate buffered saline as a control, (B) Treated with FBN.

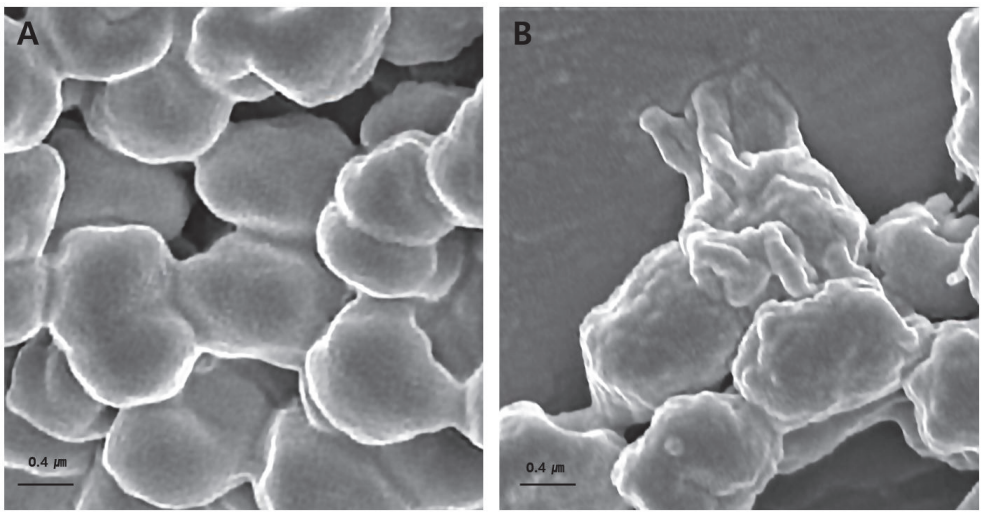

Figure 7. Cell viability of NO-releasing compound on HGF-1 cells. Cell viability of 2 mM FB and 1 mM FBN group was calculated by comparing the cell viability of the control group (100%) with that of the experimental group. (*: $p < 0.05$)

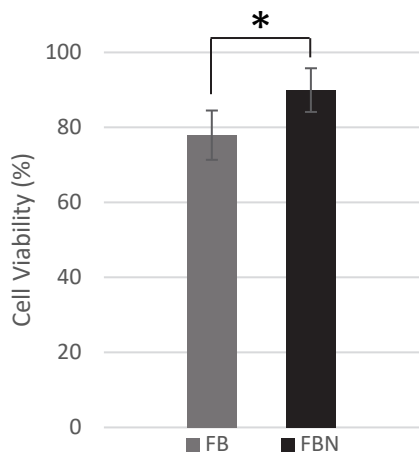

Figure 8. Representative cell migration images. Scratch analysis was performed by the method described above using HGF-1 cells with control group and each concentration of FBN (1 mM, 0.05 mM and 0.01 mM). Images were taken at the beginning of the experiment and 24 hours. Scale bar: 1000 μm.

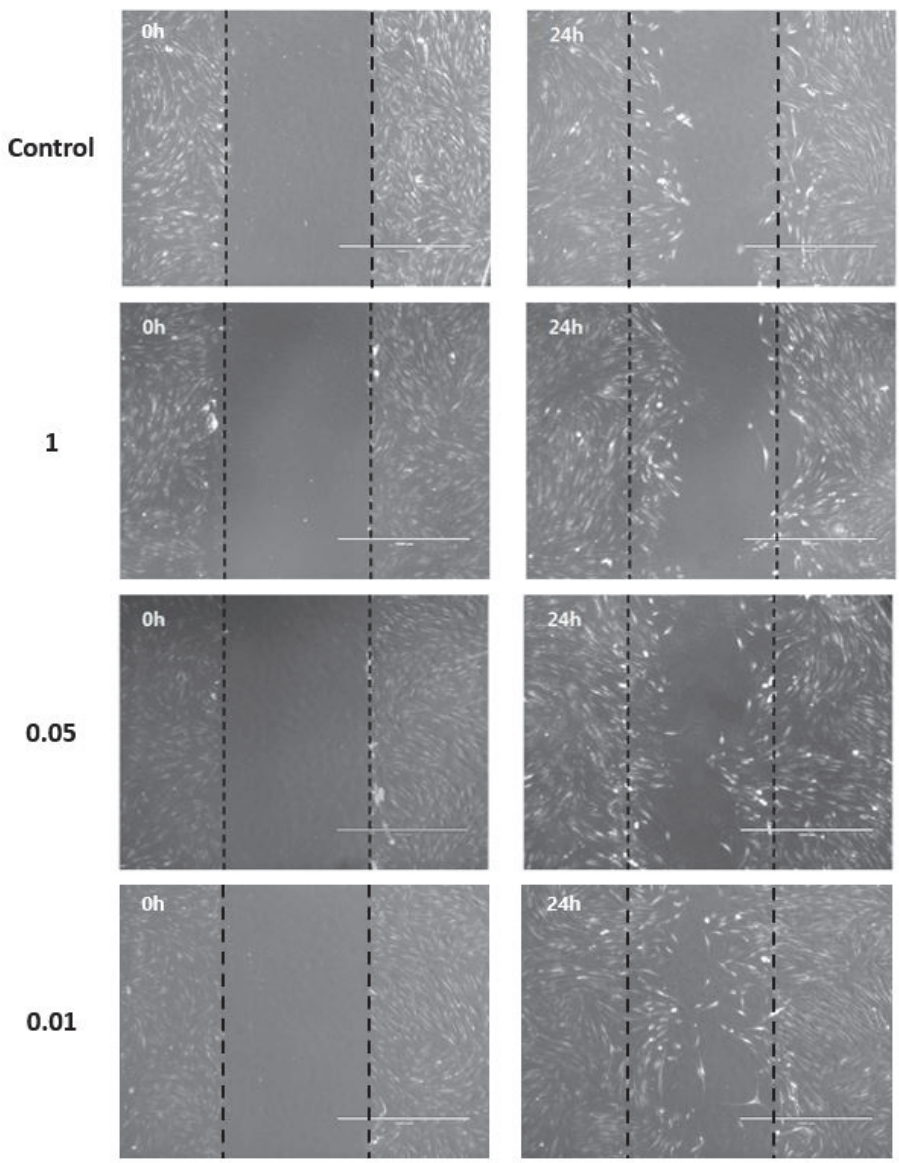

Figure 9. Migration rate of HGF-1 at control group and each concentration of FBN (1 mM, 0.05 mM and 0.01 mM). mean ± SD are shown. (*: $p < 0.05$)

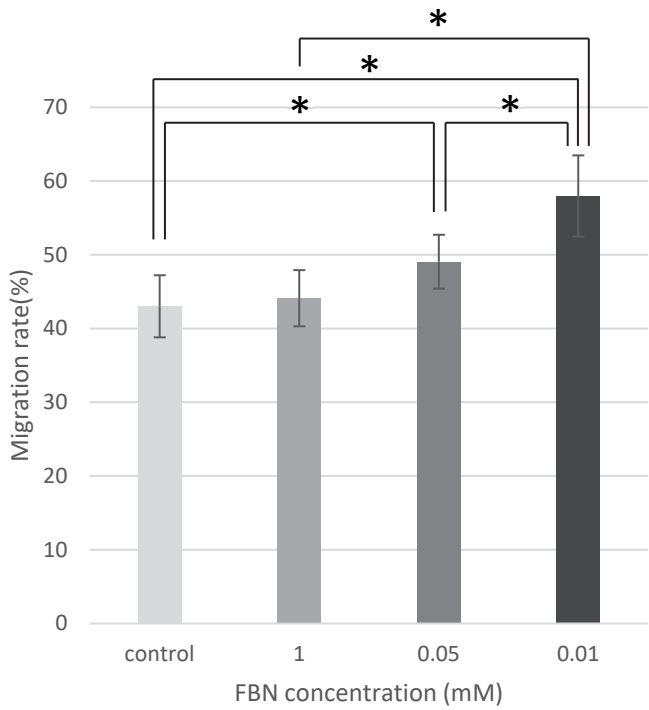

Figure 10. Representative figures of palatal wounds regeneration of three groups; control, FB (0.01 mM) and FBN (0.01 mM) in each group at 7 and 14 days after surgery.

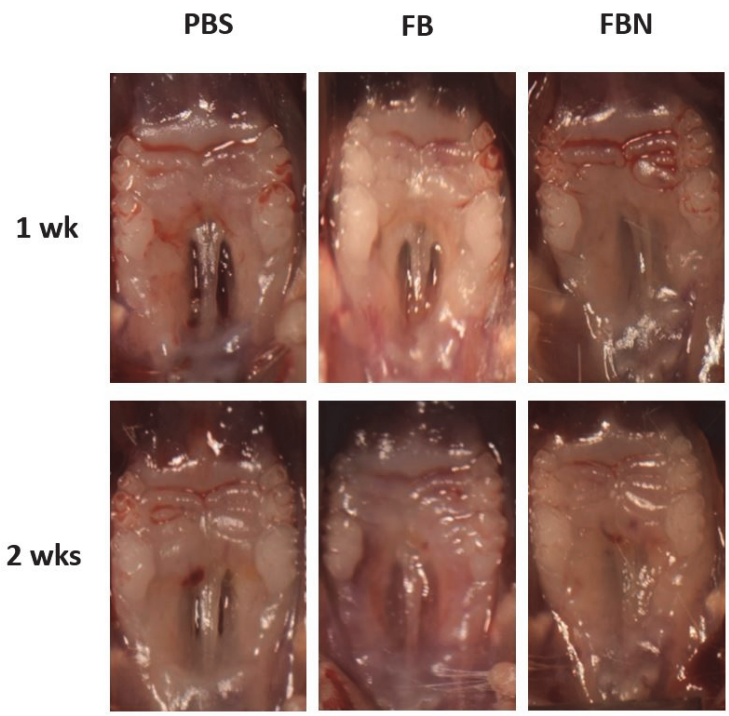

Figure 11. Effects of 0.01mM FB and 0.01 mM FBN on wound healing. The results of wound healing at 7 and 14 days after surgery are shown in graphs as percentage of wound healing area compared to day 0 in control, FB (0.01 mM) and FBN (0.01 mM). (∗: $p < 0.05$)

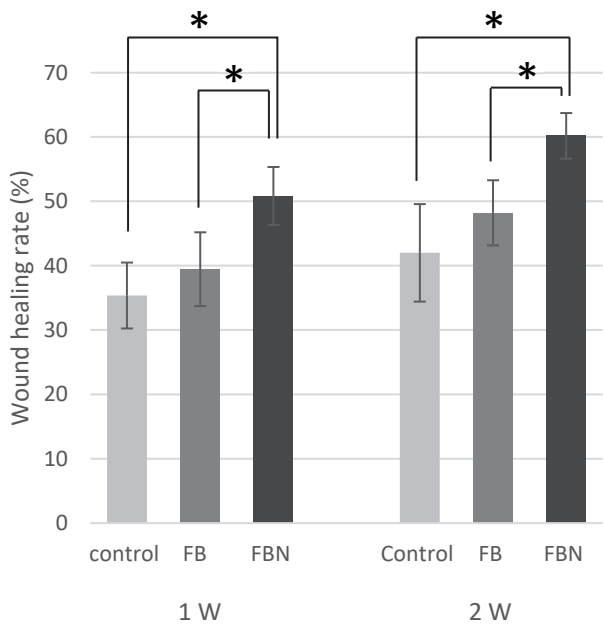

Figure 12. Images of H&E (A) and CK-14 (B) staining of wounds treated with control, FB (0.01 mM) and FBN (0.01 mM) group on day 7 and 14, respectively (X40).

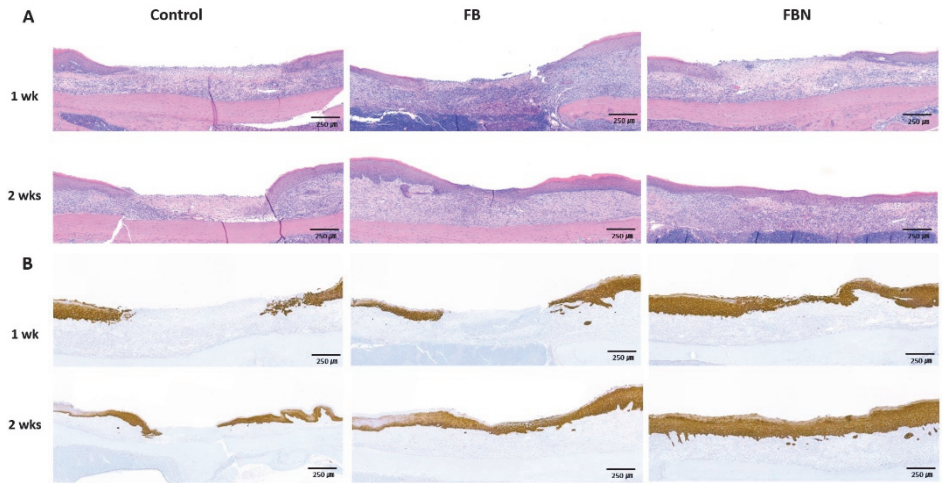

Figure 13. Images of CK-14 (A), α-SMA (B) staining of wounds treated with control, FB (0.01 mM) and FBN (0.01 mM) group on day 7 and 14, respectively (X400).

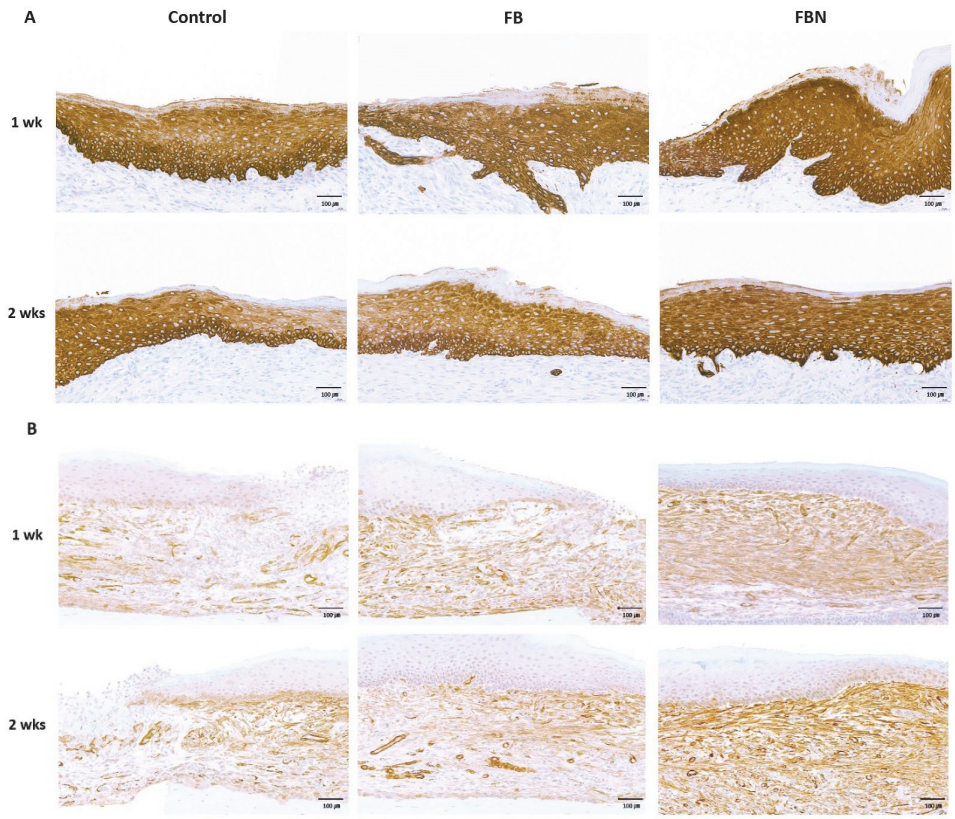

Figure 14. Representative sections view of the control, 0.05 mM FB, 0.05 mM FBN and 0.01 mM FBN group with collagen sponge at 4 weeks after surgery, respectively (A, B, C and D) and at 8 weeks after surgery, respectively (E, F, G and H), and with bone particles at 4 weeks after surgery, respectively (I, J, K and L) and at 8 weeks after surgery, respectively (M, N, O and P).

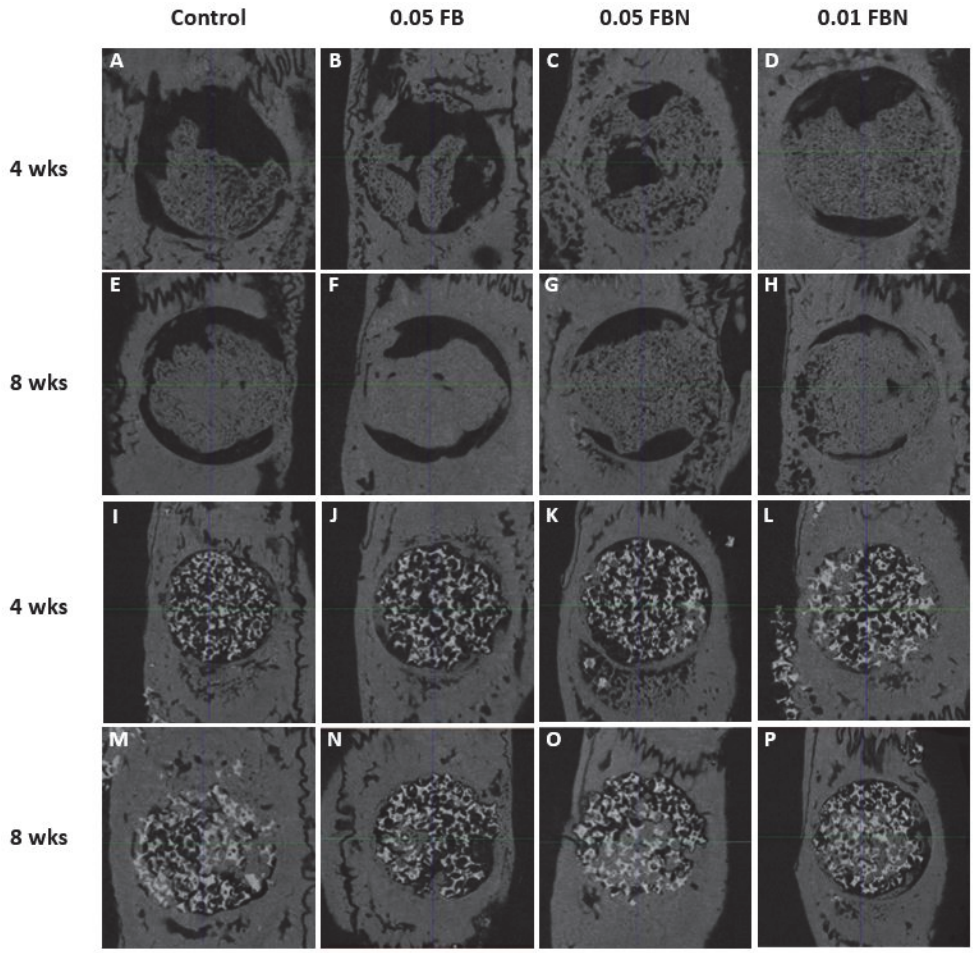

Figure 15. Bone volume fraction (BV/TV, %) in control, 0.05 mM FB, 0.05 mM FBN, 0.01 mM group with collagen sponge (A) and bone particle (B). (∗: $p < 0.05$)

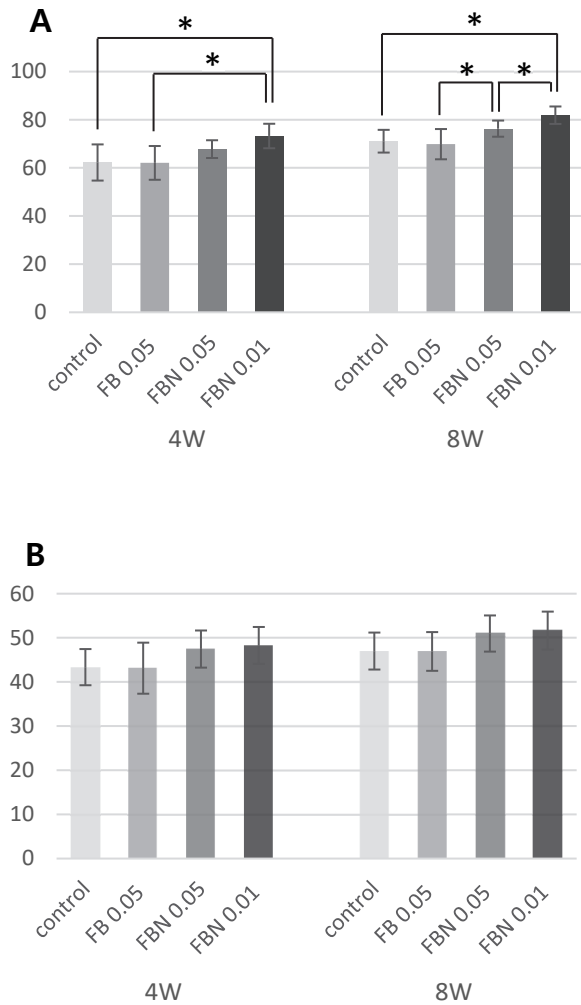

Figure 16. Bone healing parameters in each group with collagen sponge at 4 and 8 weeks after surgery. A. Number of trabeculae (Tb N); B. Trabecular separation (Tb Sp); C. Trabecular thickness (Th Th). (*: $p < 0.05$)

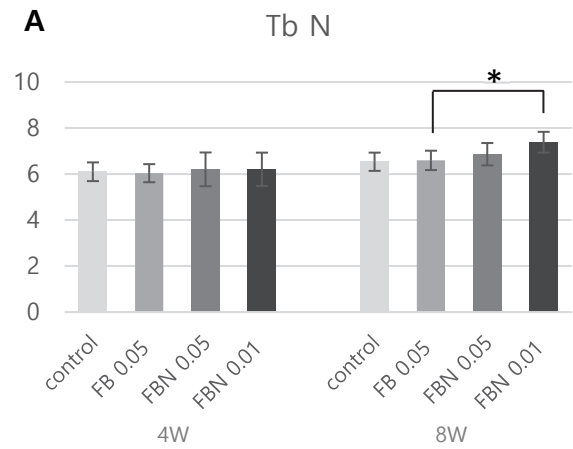

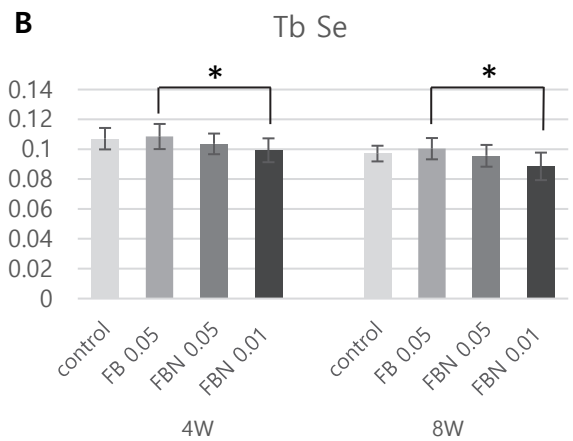

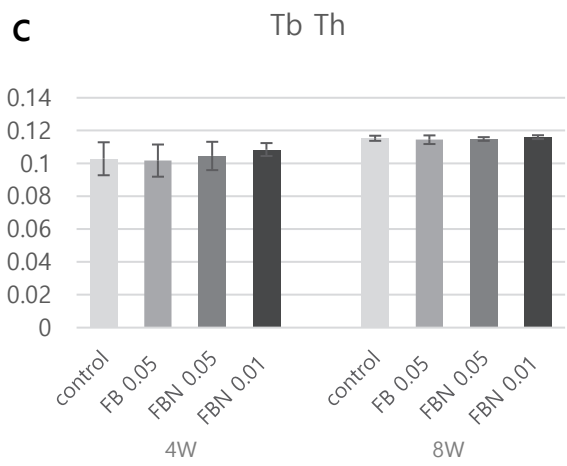
C
Tb Th
0.14
0.12
0.1
0.08
0.06
0.04
0.02
0
control
FB 0.05
FBN 0.05
FBN 0.01
control
FB 0.05
FBN 0.05
FBN 0.01
4W
8W

Figure 17. Bone healing parameters in each group with bone particle at 4 and 8 weeks after surgery. A. Number of trabeculae (Tb N); B. Trabecular separation (Tb Sp); C. Trabecular thickness (Th Th). (*: $p < 0.05$)

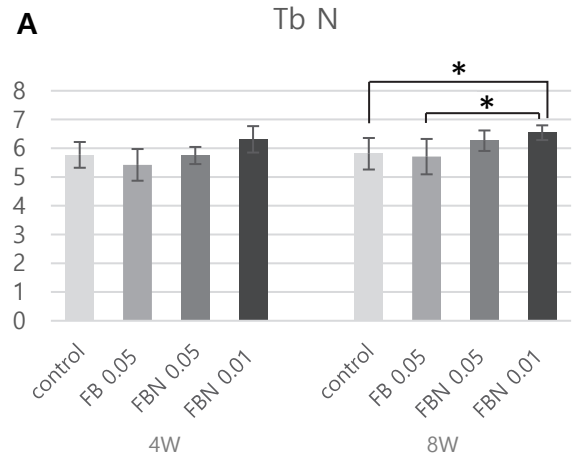

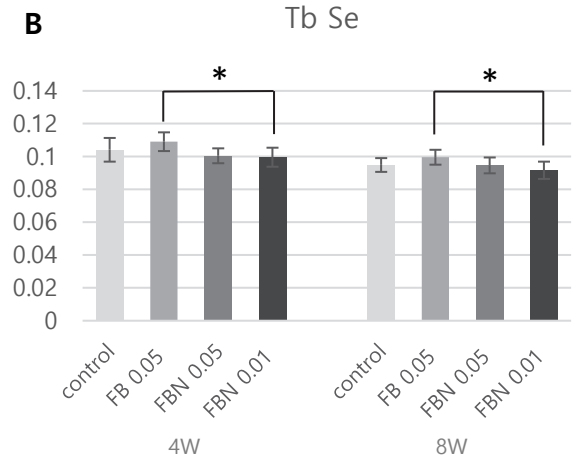

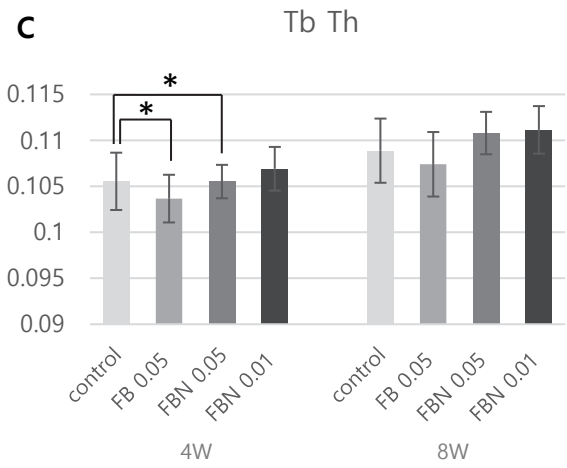
C
Tb Th
*
*
0.115
0.11
0.105
0.1
0.095
0.09
control
FB 0.05
FBN 0.05
FBN 0.01
control
FB 0.05
FBN 0.05
FBN 0.01
4W
8W

Figure 18. Representative histologic view of the control, 0.05 mM FB, 0.05 mM FBN and 0.01 mM FBN group with collagen sponge at 4 weeks after surgery, respectively (A, B, C and D) and at 8 weeks after surgery, respectively (E, F, G and H), and with bone particle at 4 weeks after surgery, respectively (I, J, K and L) and at 8 weeks after surgery, respectively (M, N, O and P) at X40 magnification.

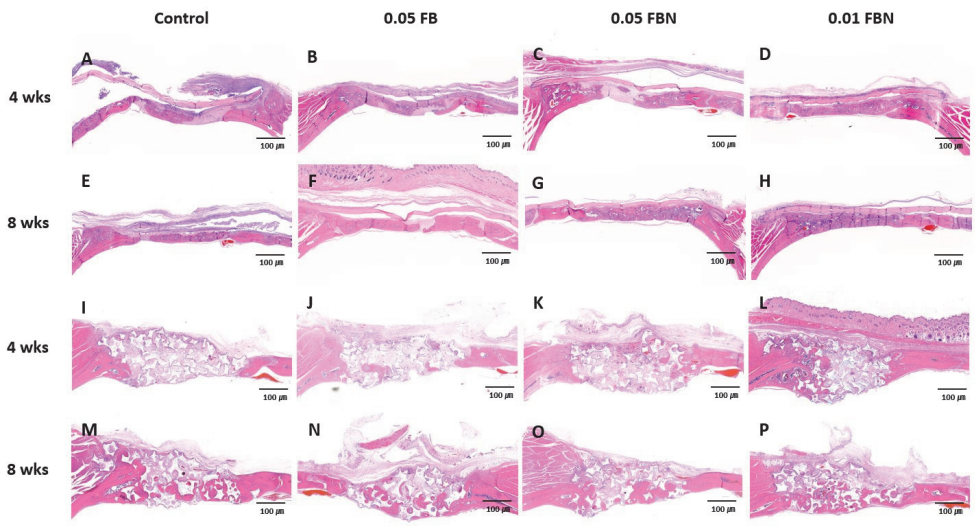

Figure 19. CD-31 stained images of the control, 0.05 mM FB, 0.05 mM FBN and 0.01 mM FBN group with collagen sponge at 4 weeks after surgery, respectively (A, B, C and D) and at 8 weeks after surgery, respectively (E, F, G and H), and with bone particle at 4 weeks after surgery, respectively (I, J, K and L) and at 8 weeks after surgery, respectively (M, N, O and P) at X400 magnification.

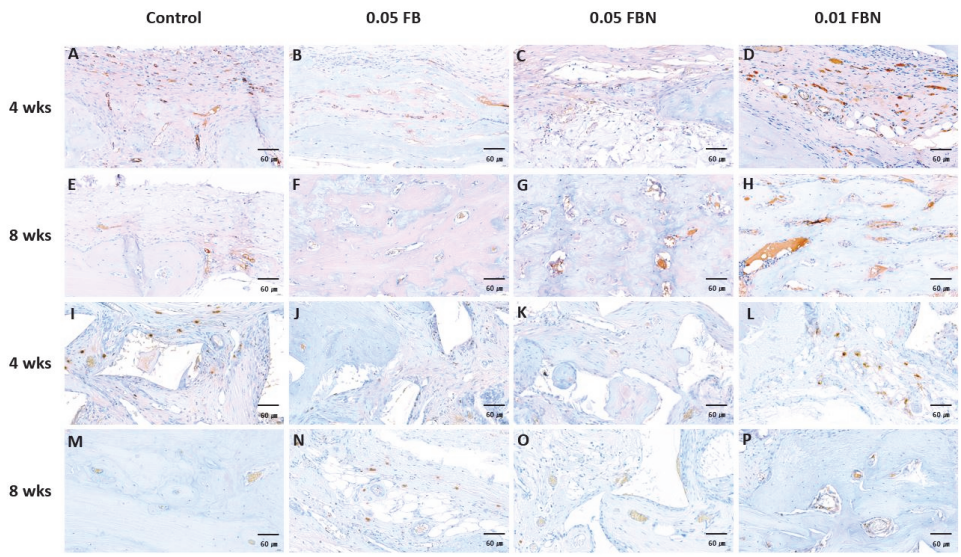

-국문초록-

연조직 및 경조직 재생에서 일산화질소 복합체의 역할

신 정 현

서울대학교 대학원 치의과학과 구강악안면외과학 전공

(지도교수 명 훈)

연구 목적

구강 내의 조직 결함은 흔히 접할 수 있지만, 치료에 종종 어려움을 겪는다. 일산화질소 복합체는 재상피화, 혈관 형성 및 조골세포 분화를 촉진함으로써 상처 치유를 향상시키는 것으로 보고되었다. 이 연구의 목적은 *in vitro* 실험과 *in vivo* 실험을 통해서, 합성된 일산화질소 복합체의 효과에 대하여 알아보는 것이다.

연구 방법

플루로닉 F68, 폴리에틸레니민 및 NONOates (FBN)로 합성된 일산화질소 복합체의 항균 효과를 평가하기 위해, FBN을 *Porphyromas gingivalis (P. gingivalis)*에 적용하였다. 또한 FBN으로 처리된 HGF-1의 이동을 평가하기 위해 스크래치 분석을 사용하였다. 구개 창상에서 FBN의 효과를 평가하기 위해 총 33마리의 BALB/C 생쥐를 사용하였다. 골결손부에서 FBN의 골재형성에 대한 역할을 평가하기 위해서, 두개골을 결손 시킨 총 80마리의 Spraque-Dawley 백서를 실험에 사용하였다. 동물 실험에서 조직학적 분석, 마이크로 CT 분석, 면역화학분석을 시행하였다.

연구 결과

플루로닉 F68-폴리에틸레니민 (FB)의 항균 작용은 관찰되지 않았지만, *P. gingivalis*의 증식을 막는 효과는 관찰되었다. FBN의 항균 및 정균 효과가 FB 보다 적은 농도에서 관찰되었다. 또한 FBN으로 처리된 HGF-1 세포에서 높은 이동률이 관찰되었고, FBN으로 처리된 군에서 상처 크기가 유의하게 감소하였다 (all $p < 0.05$). 면역화학염색에서 FBN으로 처리된 점막 상처에서 재상피화 및 상처 수축이 증가되었다. FBN과 콜라겐 스펀지를 적용한 실험 군에서 bone volume 및 bone

volume/tissue volume이 현저히 높게 측정되었다 ($p < 0.05$). CD31의 면역화학염색과 미세혈관 밀도 분석 (microvessel density, MVD)에서, 혈관신생은 FBN으로 처리된 군에서 더 두드러지게 관찰되었다.

결론

FBN은 *P. gingivalis*에 대한 항균 효과가 나타났고, HGF-1의 이동과 구개 점막 치유를 향상시켰다. 두개골 연구에서, FBN은 콜라겐 스펀지와 함께 적용하였을 때, 골 형성 촉진 효과를 나타내었다. 따라서 FBN은 궤양성 구개 점막 병소와 골이식을 할 수 없는 골 결함 부위에 콜라겐 스펀지와 함께 적용될 수 있을 것으로 사료된다.

주요어: 일산화질소, 플루로닉 F68-폴리에틸레니민-NONOates (FBN), 연조직 재생, 골재형성

학 번: 2015-30629